



Energy, Mines and
Resources Canada

Énergie, Mines et
Ressources Canada

Earth Physics Branch

Direction de la physique du globe

1 Observatory Crescent
Ottawa Canada
K1A 0Y3

1 Place de l'Observatoire
Ottawa Canada
K1A 0Y3

**Geothermal Service
of Canada**

**Service géothermique
du Canada**

INTERNAL STRESSES IN SOILS DURING FROST HEAVING

**P.J. Williams and J.A. Wood
Carleton University
Ottawa, Ontario**

**Earth Physics Branch Open File Number 85-15
Dossier public de la Direction de la Physique du Globe No. 85-15**

NOT FOR REPRODUCTION

REPRODUCTION INTERDITE

**Department of Energy, Mines and
Resources Canada
Earth Physics Branch
Division of Gravity, Geothermics
and Geodynamics**

**Ministre de l'Énergie, des Mines
et des Ressources du Canada
Direction de la physique du globe
Division de la gravité, géothermie
et géodynamique**

This document was produced
by scanning the original publication.

Ce document est le produit d'une
numérisation par balayage
de la publication originale.

ABSTRACT

A frost heaving cell with pressure-sensing apparatus was specially designed to measure the internal frost heaving pressures at different locations in a soil sample. Whereas conventional cells measure the heaving pressure generated by the entire sample, this new apparatus allows detection of differences in stress within the soil arising from temperature differences. A detailed description of the apparatus and experimental procedures is presented. Results from tests with two soil types indicate that internal stresses are not uniform during freezing. The work suggests that creep and strength properties of frozen material modulate the rate of secondary heaving and determine the effective frost heaving pressure.

RÉSUMÉ

Une cellule de gonflement au gel équipée de sondes mesurant la pression interne à différents endroits dans un échantillon a été conçue. Cet appareil permet la détection de différences de contraintes à l'intérieur d'un sol, créées sous des gradients thermiques; les cellules conventionnelles ne mesurent que la pression de gonflement exercée par l'échantillon en entier. L'appareil et la mode opératoire sont décrits en détail dans le rapport. Les résultats d'essais sur deux sols indiquent que les pressions internes ne sont pas uniformes lors du gel. L'interprétation des résultats suggère que le gonflement secondaire est modulé par le fluage et la résistance du sol gelé, et que ces propriétés contrôlent la pression effective de gonflement au gel.

INTERNAL STRESSES IN SOILS DURING FROST HEAVING

FINAL REPORT

to the

Earth Physics Branch
Department of Energy Mines and Resources

P.J. Williams
Principal Investigator

J.A. Wood
Research Assistant

Geotechnical Science Laboratories
Department of Geography
Carleton University
Ottawa, Ontario
K1S 5B6

Contract Serial No OSU83-00125
DSS File No 24SU 23235-3-1098

September, 1984

Internal Stresses in Soils
during Frost Heaving

September, 1984

TABLE OF CONTENTS

	page
INTRODUCTION	
1. APPARATUS	
1.1 General	1
1.2 Pressure - Sensing Instrumentation	1
1.3 Frost Heaving Cell	6
1.4 Temperature Control and Measurement	6
1.5 Water Supply	7
1.6 Temperature Record	8
1.7 Flow Record	8
1.8 Pressure Record	9
2. PROCEDURE	
2.1 Soils	11
2.2 Sample Preparation and Assembly of Cell	11
2.3 Nucleation and Freezing	15
2.4 Cold Reservoir	15
2.5 Frost Line	16
3. ANALYSIS	
3.1 General	18
3.2 Uptake and Discharge of Water During Heaving	18
3.3 Internal Pressures	21
3.4 Discrepancies	22
3.5 Changes to the Thermal Gradient	23
4. INTERPRETATION	
4.1 Temperature and Heaving Pressure	32
4.2 Physical Manifestation of Frost Heave	34
4.3 Role of Yield Stress in Determining Frost Heaving Pressures	35
4.4 Significance of the Observed Pressure Difference .	36
4.5 Effect of Yielding	39
4.6 Explanation for Water Expulsion and Positive Soil Pressures	40
4.7 Significance of Soil Compressibility	43
4.8 Effect of Temperature Gradient Changes on Internal Pressure	43
4.9 Measurement of Externally Effective Frost Heaving Pressure	48
4.10 Concluding Remarks	49
SUMMARY	50
REFERENCES	53
APPENDIX A	
APPENDIX B	
APPENDIX C	

LIST OF FIGURES

Figure		page
1.1	Cross-section of the Frost Heaving Cell	2
1.2	Schematic Diagram of the Experimental Apparatus ..	4
3.1	Temperature Profile During Frost Heaving, Experiment 29, Allendale Clay	24
3.2	Flows and Internal Pressures During Frost Heaving, Experiment 29, Allendale Clay	25
3.3	Temperature Profile During Frost Heaving, Experiment 30, Allendale Clay	26
3.4	Flows and Internal Pressures During Frost Heaving, Experiment 30, Caen Silt	27
3.5	Temperature Profile During Frost Heaving, Experiment 31, Caen Silt	28
3.6	Flows and Internal Pressures During Frost Heaving, Experiment 31, Caen Silt	29
3.7	Temperature Profile During Frost Heaving, Experiment 32A, Caen Silt	30
3.8	Flows and Internal Pressures During Frost Heaving, Experiment 32A, Caen Silt	31

LIST OF TABLES

Table		page
1.1	Pressure Transducer and Thermistor Code	3
2.1	Properties of the Soils Used in the Experiments ..	12
3.1	Pressure and Flow Data, Experiments 29-32A	19
4.1	Freezing Data, Experiments 29, 30 and 32A	41
4.2	Pressure and Flow Changes Accompanying Changes to the Temperature Gradient, Experiments 29-31 ...	44

INTRODUCTION

This report describes an investigation carried out in the laboratory, using specifically constructed apparatus of a design based on findings from a number of years of research into related phenomena. The idea of the experiments was also developed on the basis of findings in the earlier studies. The work under the present contract, which was for a period of seven months with provision for the report to be submitted six months later (thus allowing for longer investigations after the construction of the apparatus) has established the hypothesis that the creep properties of the frozen material modulate the rate of secondary frost heave. Secondary frost heave is due to the enlargement of ice lenses within already frozen ground which takes place against the resistance offered by the frozen material. The findings thus demonstrate the role of both mechanical and thermodynamic properties in the development of secondary frost heave and the associated externally-effective heaving pressures.

The work has been described in a paper submitted for publication and it has also been discussed in two seminars, one international. The findings help to explain observations, currently being made in the France-Canada pipeline ground freezing project, in which high stresses apparently unrelated to the bending or deformation of the pipe are detected locally in the ground. In addition to the significance of the findings for the analysis of stresses generated in and around pipelines in frozen ground, the findings are of importance in the clarification of secondary frost heave and small displacements now being considered of extreme importance in the construction of tracks for high speed trains. They are also likely to have application in development of highway technology for counteracting frost damage.

John A. Wood
Research Assistant

P.J. Williams
Principal Investigator

1. APPARATUS

1.1 General

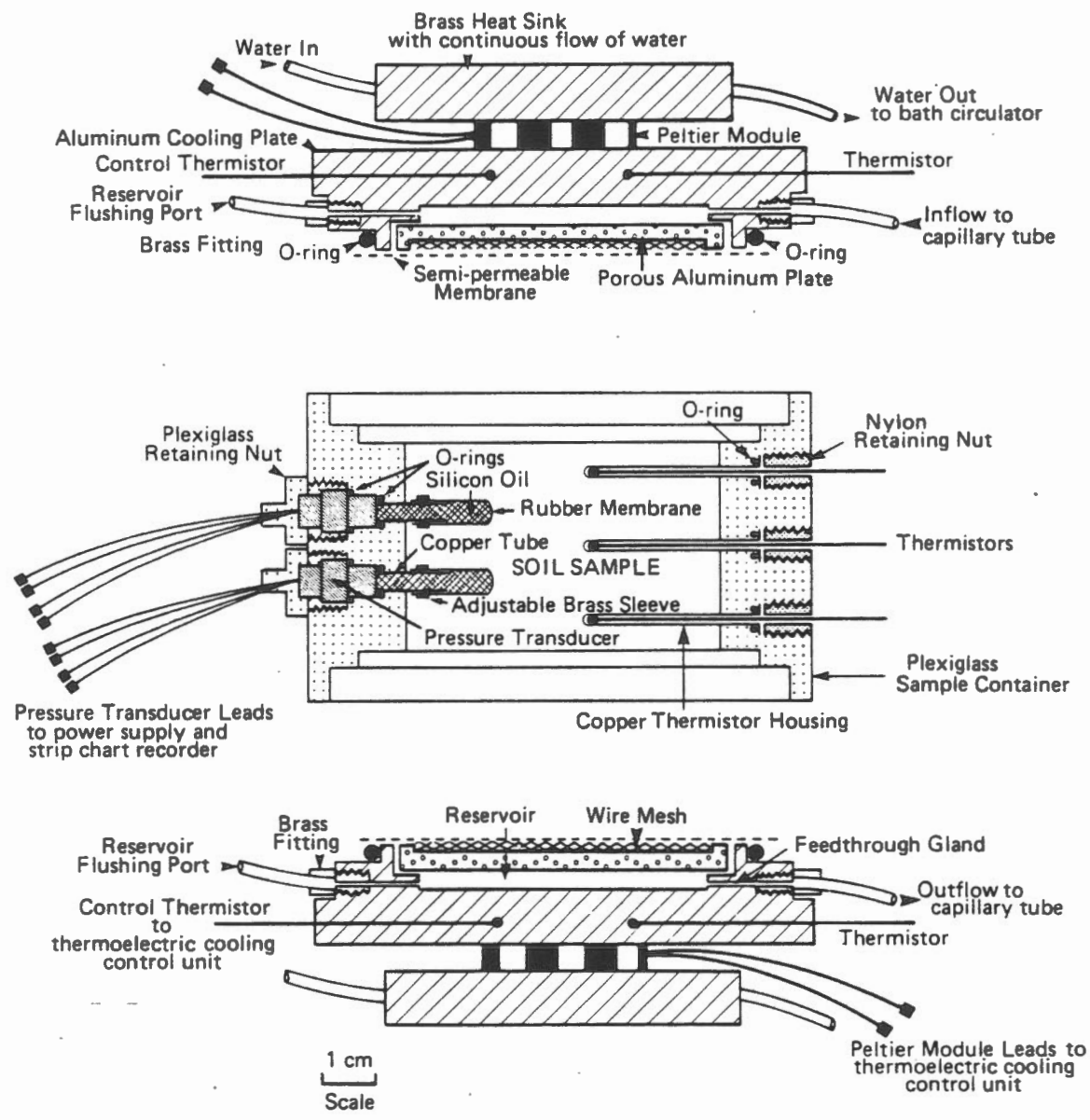
The frost heaving cell and pressure-sensing apparatus shown in Figures 1.1 and 1.2, evolved on a trial and error basis from tests conducted over several years. The experiment represents a unique approach to measuring frost heaving pressures. Firstly, it is the internal frost heaving pressure which is measured, and at different locations within the soil, rather than the heaving pressure generated by the entire sample as is done in conventional frost heaving tests. The advantage of this is that it allows detection of differences in stress occurring within the soil as a result of temperature differences, instead of a single value for the frost heaving pressure. Internal stress differences also indicate the effect of the soil strength in determining the distribution of the stress between successive ice lenses in the intervening layers of frozen soil. Furthermore, there is some uncertainty over whether conventional test results are representative of the effective heaving pressure.

An additional advantage with the design of this cell is that it is also open to water flow at both ends of the soil, which more closely simulates natural conditions. In conventional tests, water is not permitted to flow in or out of the soil at the cold end.

1.2 Pressure-Sensing Instrumentation

Pressures generated within the soil are measured with two small pressure transducer assemblies spaced 1.20 cm apart and 1.15 cm from

Figure 1.1
CROSS-SECTION OF THE CELL



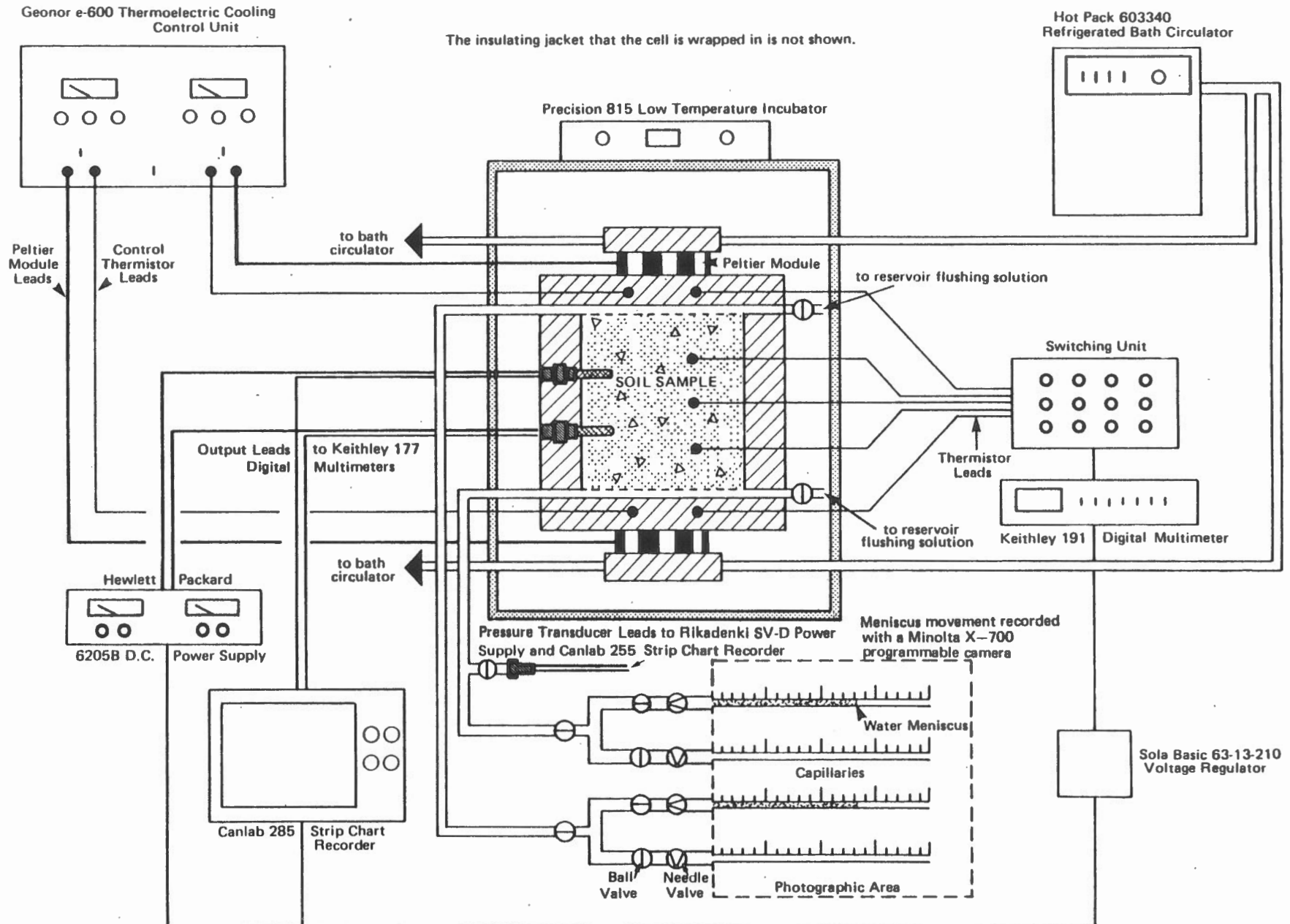
The steel clamp and nylon screws used to hold the apparatus together are not shown. Brass fittings and plexiglass retaining nuts are not drawn to scale.

TABLE 1.1

Pressure Transducer and Thermistor Code

T ₁	Cooling Plate thermistor, 1.50 cm from E ₁
E ₁	Boundary of soil sample, 3.50 cm from E ₂
T ₂	Soil thermistor, 1.985 cm from T ₁ 0.50 cm from E ₁
P ₁	Transducer, 1.15 cm from E ₁ , 1.20 cm from P ₂ (0.65 cm from T ₂ , 0.60 cm from T ₃)
T ₃	Soil thermistor, 3.235 cm from T ₁ , 1.75 cm from E ₁ and E ₂
P ₂	Transducer, 1.15 cm from E ₂ (0.60 cm from T ₃ , 0.65 cm from T ₄)
T ₄	Soil thermistor 4.485 cm from T ₁ , 0.50 cm from E ₂
E ₂	Boundary of soil sample, 3.50 cm from E ₁
T ₅	Cooling plate thermistor, 1.50 cm from E ₂

Figure 1.2
SCHEMATIC REPRESENTATION OF THE ENTIRE EXPERIMENT



the 'warm' and 'cold' ends of the soil sample. The transducers (Kulite VQS-250 type, rated pressure = 50 psi, 350 kPa) are mounted so that their entire length is accommodated in the walls of the cell, to minimize potential external thermal disturbances.¹ (Calibration reports are given in Appendix A): The transducers press against small copper tubes which extend 1.1 cm into the soil over which are fitted small oblong rubber membranes. The surface area of each membrane sensitive to pressure changes is about 1.8 cm². Seals are made by small o-rings and a miniature adjustable brass sleeve. The membranes are filled with Dow Corning 200 dimethyl silicone oil (freezing temperature = -50°C, viscosity = 350 centistones at 25°C, compressibility = 0.01%/100 kPa).

In last year's report some difficulty with the pressure-sensing apparatus was mentioned (Torrance and Wood, 1983). This involved the formation of stress cracks emanating from the flange of the copper tubes and extending to the inner wall of the cell as a result of overtightening of the plexiglass-retaining nuts. The problem was eliminated by machining the cell to precise dimensions so that only a finger-tight torque is required to make a seal at pressures over 400 kPa (4 atm). The other problem concerned damage to the pressure transducer leads at the back of the steel casing as a result of bending during handling and assembly of the cell. As a preventative measure

¹ The transducer retaining nuts are too large for the transducers to be aligned vertically along the axis of the cell. Because of this they are offset by a 45° angle, about 4 cm apart on the outer wall of the cell.

small plexiglass tubes 2 cm long have been added to the back of the transducer-retaining nuts to guard against excessive bending of the leads.

1.3 Frost heaving Cell

The cell comprises a plexiglass cylinder containing the soil sample (diameter = 5.4 cm, length 3.5 cm), the temperature of which is controlled by two aluminum cooling plates at either end of the soil. The cooling plates are attached to the sample container by 12 nylon screws. A large steel clamp was added as a precautionary measure to prevent small volume changes which might otherwise occur due to elastic strain of the nylon screws under stress.²

1.4 Temperature Control and Measurement

The system is cooled by Peltier modules and a thermoelectric cooling control unit accurate to $\pm 0.005^{\circ}\text{C}$. Soil temperatures are obtained from three YSI 3000A thermistors housed in copper tubes with seals to prevent pressure loss within the cell. The tips of the thermistors are coated with heat-conducting grease to ensure thermal contact with the copper housings.

The cell is wrapped in a jacket of foam rubber insulation 15 cm thick, and placed inside a Precision low-temperature incubator, set at $0^{\circ}\text{C} \pm 0.1^{\circ}\text{C}$. This eliminates radial heat exchange with the surroundings, ensuring that the temperature gradient across the soil is

² Nylon screws are used instead of steel to prevent excessive cooling of the cell walls which disrupts the linear temperature gradient within the soil.

linear. Two small fans are located at either end of the cell, circulating cool air from the incubator toward the cell and warmer air produced by the brass heat sinks away from the cell.

1.5 Water Supply

Both ends of the sample are in contact with small reservoirs containing distilled water from which the soil imbibes or expels water according to gradients of chemical potential within the soil pores. When the reservoir temperature is below 0°C, a lactose solution is used instead of pure water because, (i) it prevents the water from freezing in the reservoirs and (2) it lowers the chemical potential of the water and eliminates potential osmotic gradients between the reservoirs and the soil. The solute concentration is the amount required to equalize the chemical potential of the water in the reservoirs and that in the adjacent soil (solid and liquid phases), at the prevailing temperature.³

A cellulose acetate membrane (pore diameter < 0.005 μ m, freezing temperature -6°C) separates the soil from the reservoirs. The membranes readily transmit water but restrict the entry of lactose. To prevent deflection of the membranes under pressure they are supported by porous aluminum plates in which vertical holes 0.2 cm diameter are drilled 0.25 cm apart. A recent addition includes a disc of wire mesh which is located inside a shallow indentation in each plate and presses against the membrane. This ensures that water is in

³ The required solute concentration at a specified temperature is obtained from freezing-point depression tables for lactose.

contact with the membrane over its entire surface area. It also facilitates circulation of the fluid in the reservoir during flushing.⁴

1.6 Temperature Record

Temperature measurements are made manually at regular intervals during the first 4-6 hours of each test when the temperature change is most rapid. Steady-state conditions are normally achieved about 48 hours after freezing is initiated. After the initial period, temperature readings are made every 24 hours and minor adjustments are made to the thermoelectric cooling control unit to maintain constant temperatures. Temperature readings are accurate to within 0.0025°C.

1.7 Flow Record

A continuous record of water intake and expulsion by the soil is made by photographing the movement of a water meniscus in glass capillaries (0.184 cm internal diameter) at regular intervals with a Minolta X-700 programmeable camera. A cross-feed network of copper tubing, brass ball and needle valves and tee junctions mounted on a steel plate connects the capillaries to the reservoirs and allows the capillaries to be removed or changed without interruption to the flow record. The capillaries are filled with a red dye (propylene glycol)

⁴ In previous years, plates made of sintered brass were used as membrane supports instead of the present set-up. The plates were saturated by boiling them in the appropriate lactose solution prior to assembly of the cell. However, if temperature changes required a change in lactose concentration, flushing the reservoir presented a serious difficulty because the solution could not be readily replaced in the plate owing to its small pores.

and are located on a finely divided scale with a white background to enhance contrast on the film. A small quantity of water is injected into the tip of each capillary to prevent evaporation of water from the meniscus.

The camera is mounted on a steel framework 1 m above the capillaries. Negatives are developed in the laboratory darkroom and flow readings are deciphered with the aid of a microfilm projector. The film resolution allows the meniscus position to be determined within $\pm 0.10\text{cm}$, hence the potential error in a flow reading is $\pm 0.0027\text{ cm}^3$.

1.8 Pressure Record

Soil pressures are monitored by a Canlab 285 strip-chart recorder. Before each experiment, the recorder must be calibrated to accommodate the anticipated range of stress occurring within the soil, as well as the sensitivity of each transducer. In general, values indicated by the recorder are accurate to within $\pm 2.5\text{ kPa}$.

The input voltage to the pressure transducers is 1 V.d.c. At this level, their sensitivity is approximately 0.026 mV kPa^{-1} . There is a slight heating effect caused by the high resistance of the wheatstone bridge. At 1 V.d.c., this was found to be 0.015°C within 0.1 cm of the transducer diaphragms. However, this should not have a significant effect on the soil temperature since the heat flow is reduced by the oil and rubber membranes and the rate of heat extraction from the cell is very large (approximately, 170 Jhr^{-1}).

The transducers are sealed with an internal reference pressure.⁵ Because of this, changes in the atmospheric pressure are detected by the transducers and incorporated into the results. Although atmospheric pressure may change by as much as 5 kPa, the daily change rarely exceeds 2 kPa.

⁵ Originally, atmospheric referenced transducers were used, but were discontinued owing to handling difficulties caused by the steel tubes emerging from the back of the steel casing. Bending of these tubes when the cell was wrapped in insulation caused damage to some transducers.

2. PROCEDURE

2.1 Soils

Frost heaving tests have been carried out using two different kinds of soil, (1) Allendale clay, which was used in previous experiments, and (2) Caen silt. The former is a colloidal material containing slightly less than 50% clay and a high percentage of silt. In its natural state, it is well flocculated having spheroidal aggregates 0.1 cm in diameter which explains its relatively low bulk density and high saturated moisture content and permeability (unfrozen). Caen silt is an inorganic non-colloidal soil with a granular (non-cohesive) structure, which is currently being used at the controlled environment facility, Caen, France in the Canada-France pipeline freezing project (Guichaoua and Williams, 1984). Properties of both of these soils are listed in Table 2.1.

2.2 Sample Preparation And Assembly of Cell

Careful attention has been given to the preparation of the soil samples since this could have a significant effect on the results obtained. In each of the tests, with the exception of experiment 31, the soil was saturated with distilled water and placed in a vacuum chamber for 30 minutes to remove entrapped air from the pores. The soil was then decanted into the partially assembled cell and allowed to consolidate under its own weight for 24 hours. Gentle suction removed any supernatant liquid from the surface of the soil and further small quantities of soil were added until the sample container was deemed

TABLE 2.1
Properties of the Soils Used in the Experiments

	Grain Size Distribution			USDA Classification
	% sand (>50 μ m)	% silt (50-2 μ m)	% clay (<2 μ m)	
Caen	30.4	56.5	13.1	silt
Allendale	17.7	33.9	48.5	clay

Mineralogy

Caen Silt	Chiefly quartz with small amounts of chlorite and calcite.
Allendale Clay	Illite and chlorite present in large amounts. Smaller amounts of quartz, plagioclase and orthoclase feldspar and traces of amphiboles.

Physical Properties

	Caen Silt	Allendale Clay
ρ_B	1.5	1.2
ρ_s	2.67	2.68
W	$\approx 26\%$	$\approx 43\%$
θ	$\approx 39\%$ (at $\rho_B = 1.5 \text{ g cm}^{-3}$)	$\approx 39\%$ (at $\rho_B = 1.27 \text{ g cm}^{-3}$)
K_{uf}	1×10^{-7} to 5×10^{-8} (at $\rho_B = 1.73 \text{ g cm}^{-3}$)	8×10^{-3} (at $\rho_B = 1.2 \text{ g cm}^{-3}$)
λ_{uf}	1.97	1.04
C_{uf}	0.27×10^7	0.29×10^7
$\lambda_{f(T=-0.3^\circ\text{C})}$	≈ 1.7	≈ 0.7
$C_{f(T=-0.3^\circ\text{C})}$	--	0.4×10^7

ρ_B = bulk density (naturally occurring), g cm^{-3}

ρ_s = particle density, g cm^{-3}

continued

TABLE 2.1 (continued)

W	=	saturated water content (gravimetric), % dry wt.
θ	=	saturated water content (volumetric), % total vol.
K_{uf}	=	hydraulic conductivity, unfrozen (saturated), cm s^{-1} .
λ_{uf}	=	thermal conductivity, unfrozen state, (saturated) $\text{Wm}^{-1} \text{K}^{-1}$
C_{uf}	=	volumetric heat capacity, unfrozen (saturated), $\text{Jm}^{-3} \text{K}^{-1}$
$\lambda_{f(T=-0.3^\circ\text{C})}$	=	thermal conductivity, frozen (saturated), $\text{Wm}^{-1} \text{K}^{-1}$
$C_{f(T=-0.3^\circ\text{C})}$	=	volumetric heat capacity, frozen (saturated), $\text{Jm}^{-3} \text{K}^{-1}$

'exactly full'. Next, the other end plate with membrane was attached and the 'warm' reservoir was purged with distilled water.¹

In experiment 31, the soil was compacted to a very high density (1.70 g cm^{-3}) which approximates the value for the soil used in the Caen project in France (1.73 g cm^{-3}). The following procedure was used.

Proctor compaction curves predict a maximum density of 1.80 g cm^{-3} is obtained by compacting the soil at 15% water content (dry wt.). Since the volume of the cell is 80.2 cm^3 , the required amount of dry soil at this density is $80.2 \text{ cm}^3 \times 1.7 \text{ g cm}^{-3} = 136.3 \text{ g}$. The soil was weighed out and wetted with 20.5 g of water to give a water content of 15%. The soil was then packed into the partially assembled cell using a tamping rod, care being taken to ensure that the packing was as uniform as possible. A porous stone was placed over the open end of the sample, the cell was clamped and the reservoir in the cooling plate at the other end of the soil was filled with water. Next, air was purged from the soil pores by applying 400 kPa hydraulic pressure to the reservoir forcing water to flow up into the soil displacing the air. Saturation was indicated by the presence of water oozing through the porous stone at the upper end of the sample.

Although saturation was assumed, it appears that some air was still trapped in the soil pores. The predicted water content for saturation at a density of 1.70 g cm^{-3} is 21.3%, whereas the actual

¹ Prior to assembly, the cellulose acetate membranes, which are stored in a solution of 25% ethanol and water, are washed in distilled water for 24 hours, to remove all traces of alcohol from the pores. During assembly of the cell, care is taken to ensure that the membranes do not dry out as this will irreversibly damage their pore structure.

value was 18.7% (dry wt.). The discrepancy indicates that 3.52 cm^3 or 4.4% by volume of air remained in the soil pores. Although this is a relatively small quantity of air, it probably has a significant effect on the results obtained by generating a counter-suction which reduces the frost heaving pressure.

2.3 Nucleation and Freezing

After assembly, the cell was wrapped in its jacket of insulation, clamped and placed inside the incubator, which was adjusted to 0°C . Once thermoelectric cooling control was established, the soil was brought to a uniform temperature of $+0.10^\circ\text{C}$ and allowed to equilibrate for about 24 hours. Final adjustments were made to the camera and strip chart recorder.

Freezing was initiated by momentarily lowering the temperature of one cooling plate to -3°C . Nucleation is indicated by observing the temperature at the cold end of the soil. Initially this declines rapidly indicating supercooling of the soil. After about 2-3 minutes, the temperature abruptly begins to rise as latent heat is released once freezing commences. Immediately after nucleation the cold-end temperature was quickly raised and stabilized at -0.50°C .

2.4 Cold Reservoir

The cold reservoir was not flushed with lactose until about 24 hours after freezing commenced. There are two reasons for this:

- (1) At any temperature, a unique concentration of lactose is required in order to equalize the chemical potential of the water in the

reservoir and that in the soil. However, during the initial stage of each experiment, the soil temperature is continuously changing and a thermal steady-state is not established for about 48 hours. This would necessitate almost continuous flushing of the reservoir, which is not possible.²

- (2) Ideally, the reservoir membranes are only permeable to water. However, in reality, minute quantities of lactose are able to diffuse through the membrane and thaw the soil at a very slow rate averaging about 0.03 cm day^{-1} .³ If lactose enters the soil before it is frozen, then the sugar molecules will quickly diffuse through the soil reducing overall, the amount of pore ice that would otherwise form in the soil. Since frozen soil is relatively impermeable in comparison with unfrozen soil, if the soil is allowed to freeze first, lactose penetration is limited to a very narrow zone at the cold extremity of the soil and its effect is minimized.

2.5 Frost Line

At the end of each experiment, the cell was quickly dismantled and the location of the frost line was determined with Vernier calipers. The frost line is defined as the isotherm where pore ice first occurs

² Flushing temporarily disrupts the thermal equilibrium of the soil because the solution is stored at the incubator temperature, 0°C , which is warmer than the cold end of the soil.

³ A thawed layer 0.3 cm thick was observed at the cold end of the soil after a test of 10 days duration.

in the soil. This is located some distance behind the 0°C isotherm as a result of the freezing-point depression produced by the soil solutes. The boundary between the frozen and unfrozen soil is assumed to be the point where the soil resists further penetration by the metal shaft of the Vernier calipers under a gentle pressure. In reality, the true position of the frost line may be at a slightly warmer temperature than the measured position since soil with very small quantities of pore ice may offer no significant resistance to penetration. However, the error probably does not exceed 0.2 cm maximum.

After determining the position of the frost line, the sample was dissected, examined with a hand lens and the location and thickness of any visible ice lenses was noted. Finally, the soil was weighed, dried and its moisture content and bulk density were determined.

⁴ The frost line is assumed to be located at the mean of 6 measurements taken around the perimeter of the soil sample. The measurements never differed by more than 0.3 cm and generally varied by less than 0.2 cm.

3. ANALYSIS

3.1 General

Results from four tests, two with the Allendale clay and the other two with Caen silt, are shown in Figures 3.1-3.8. All of the tests were run in exactly the same manner with a temperature gradient of $0.17^{\circ}\text{C cm}^{-1}$. (Warm end temperature $+0.10^{\circ}\text{C}$, cold end temperature -0.50°C). In general, a fairly consistent pattern of stresses and water flows was observed. There was some departure from the pattern in experiment 31 with the Caen silt which was compacted to a very high density. A summary of the results is given in Table 3.1.

3.2 Uptake and Discharge of Water During Heaving

With the exception of experiment 31, the soil discharged water from the warm end, at a diminishing rate for several hours immediately following nucleation. In the test with the Caen silt (experiment 32A), the amount of expelled was almost twice as large as that by the Allendale clay ($Q_e(t_2)$, Table 3.1). The uptake of water by the warm end began about 15 hours after freezing was initiated and continued for the remainder of the test, provided the temperature of the soil was not changed. The uptake was considerably less than the initial expulsion and occurred at a much slower rate. The rate of intake was fairly rapid initially but declined to an exceedingly low rate over a period of several days, approaching a zero flow condition.

At the cold end of the soil, the flow was much smaller than at the warm end and also less predictable. In all of the tests except

TABLE 3.1
Pressure and Flow Data, Experiments 29-32A

Experiment Soil	29 Allendale	30 Allendale	31 Caen	32A Caen
ρ_B	1.07	1.27	1.70	1.32
n	60.1	52.6	36.2	50.5
w	48.3	38.7	18.7	38.3
θ	51.7	49.1	31.8	50.6
$Q_w(t_1)$	0.37(190)	0.52(284)	-1.13(168)	1.22(406)
$Q_c(t_1)$	-0.27(190)	0.10(284)	0.24(168)	-0.26(406)
$Q_T(t_1)$	0.10(190)	0.62(284)	-0.89(168)	0.96(406)
$Q_e(t_2)$	0.84(18)	0.84(15)	0	1.59(20)
$Q_u(\Delta t)$	0.48(172)	0.32(269)	1.13(168)	0.29(386)
R	0.071	0.029	0.161	0.030
P_c	143/138	234/217	171/138	204/200
P_w	64/48	112/7	123/104	130/30
$\Delta P(t)$	91(190)	207(284)	66(15)	174(404)
Observations	hairline thickness ice lenses observed near cold end.	hairline thickness ice lenses observed near cold end.	no visible ice lenses observed.	small ice lenses (0.03-0.04 cm) thick observed in zone 1.25- 1.75 cm from cold end
ΔT	0.143	0.171	0.086	0.171
f	1.30/-0.080	0.80/-0.050	2.00/-0.065	1.08/-0.095

... continued

TABLE 3.1 (continued)

ρ_B	bulk density, g cm^{-3}
n	porosity, %
W	gravimetric water content, % (dry wt.)
θ	volumetric water content, % (total volume)
$Q_w(t_1)$	net flow, warm end, cm^3 , at time t_1 , hrs.
$Q_c(t_1)$	net flow, cold end, cm^3 , at time t_1 , hrs.
$Q_T(t_1)$	$= Q_w(t_1) + Q_c(t_1)$ overall water loss or gain by the entire sample, cm^3 , at time t_1 , hrs. (Negative values indicate net gain of water by the soil. Positive values indicate net loss).
$Q_e(t_2)$	initial water expulsion, warm end, cm^3 , at time t_2 , hrs.
$Q_u(\Delta t)$	total water uptake, warm end, cm^3 , during time interval $\Delta t = t_1 - t_2$, hrs.
R	mean rate of water uptake, $\text{cm}^3 \text{ day}^{-1}$, during time interval Δt
P_c	maximum pressure, cold transducer, kPa/second value is the pressure observed at time t_1 , hrs.
P_w	maximum pressure, warm transducer kPa/second value is the pressure observed at time t_1 , hrs.
$\Delta P(t)$	maximum pressure difference observed between warm and cold end transducers, kPa, at time t , hrs.
Observations: made at end of experiment	
ΔT	final temperature gradient at end of experiment, $^{\circ}\text{C cm}^{-1}$
f	location of frost line from warm end of soil, cm/ second value is temperature at the frost line interpolated from thermal profile, $^{\circ}\text{C}$

experiment 31, there was a slow uptake of water by the cold end. In experiment 30, the cold end discharged water for two days before the intake began.

Curiously, although there was a substantial increase in pressure within the cell overall, the soil appears to have experienced a net loss of water except experiment 31 where there was a net gain ($Q_T(t_1)$, Table 3.1). The amount of this loss varied considerably from one test to the next but appears to have been significantly greater with the Caen than the Allendale soil.

3.3 Internal Pressures

During the first 3 or 4 hours of each test, pressures remained stable within a few kPa of atmospheric pressure but then started to rise sharply, in some instances by as much as 30 kPa hr^{-1} . This occurred despite the initial expulsion of water from the warm end of the sample. The pressure increased at a diminishing rate at both locations within the soil, finally reaching a peak between 3 and 7 days after freezing commenced. Peak values were not attained simultaneously, the time lag being as much as 2 days at the cold transducer.

At the cold end, the pressure stabilized and remained constant within a few kPa of its maximum value for the duration of the test. However, at the warm end, a very different pattern was observed, the pressure declining at a very slow rate following the peak and

eventually levelling off at a value near atmospheric pressure.¹ Again, experiment 31 was the exception to the pattern with regard to pressure changes.

3.4 Discrepancies

Although experiment 31 shows similarities with the other three tests, the results are unique in certain respects. The most striking difference is that there was no initial discharge of water from the warm end during freezing. Instead, there was a large uptake, the amount being comparable to the initial expulsion in experiment 32A.

Another important deviation is that the large difference in pressure between the warm and cold-end transducers which occurred in the other three tests, was much smaller. Curiously, the cold-end pressure, instead of levelling off at, or near, its peak value, declined sharply by about 80 kPa mid-way through the test, approaching the pressure at the warm end and then increased again by about 40 kPa. The pressure at the warm transducer did not show any tendency to decline significantly as occurred in the other three tests, instead remaining within a few kPa of its peak value for the remainder of the experiment.

All of the differences occurring in experiment 31 appear to be related to the fact that the soil is much less compressible than in the other three tests. The sample was compacted to a very low porosity, 36.2%, which is within 4% of its maximum value (32.5%).

¹ In experiment 29, it appears likely that the pressure at the warm transducer would have declined further if sufficient time had been allowed (See Figure 3.2).

3.5 Changes to the Thermal Gradient

The abrupt changes in pressure and water flows near the end of experiments 29, 30 and 31 are a result of deliberate changes to the temperature gradient of the soil. Raising or lowering the temperature at one end of the cell produced a corresponding decrease or increase in the pressure, the magnitude of which appears to be directly proportional to the temperature change. For example, in experiment 30, when the temperature at the warm end was raised by 0.20°C (from $+0.10^{\circ}\text{C}$ to $+0.30^{\circ}\text{C}$) this resulted in a decrease in pressure at the cold-end transducer of 62 kPa. Lowering it by 0.30°C (from $+0.30^{\circ}\text{C}$ to 0.00°C) increased the pressure by 99 kPa. The ratio of the pressure changes, $\frac{99 \text{ kPa}}{62 \text{ kPa}} = 1.6$, corresponds almost exactly with the ratio of the changes in temperature, $\frac{0.30^{\circ}\text{C}}{0.20^{\circ}\text{C}} = 1.5$, implying a mean pressure change of about 32 kPa/ 0.10°C . Similar changes were observed at the warm-end transducer although the magnitude of the pressure change was considerably less owing to the relatively warm temperatures of the soil.

Near the end of experiment 30, the temperature gradient was reversed. This resulted in expulsion of water from the warm end* (formerly the cold end) and uptake at the cold end* (formerly the warm end). Curiously, the pressures at both transducers declined to sub-atmospheric values and showed no tendency to increase, although this may have occurred eventually if the experiment had been allowed to run longer.

Figure 3.1
 Temperature Profile During Frost Heaving,
 Experiment 29, Allendale Clay

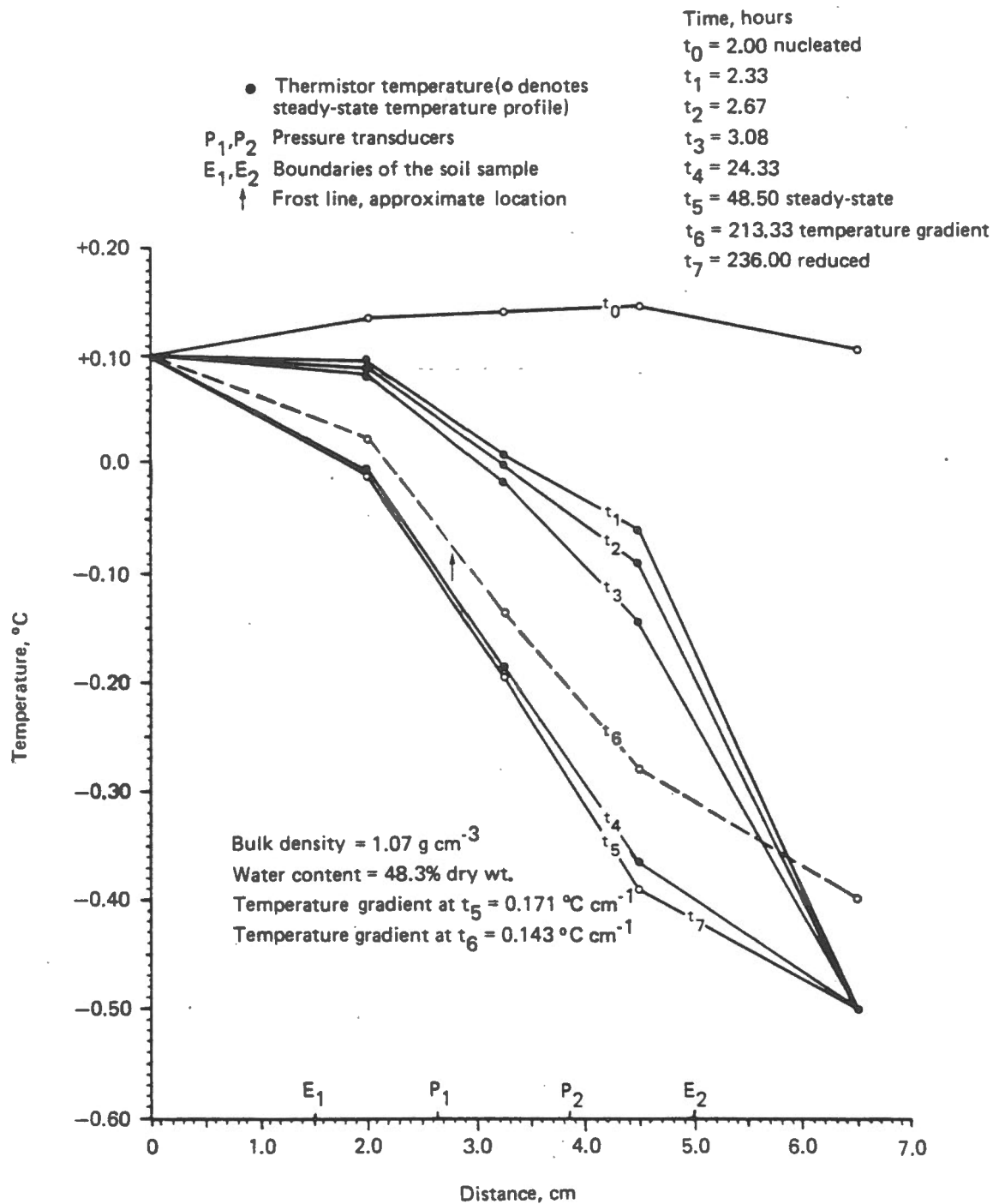


Figure 3.2

Flows and Internal Pressures During Frost Heaving, Experiment 29, Allendale Clay

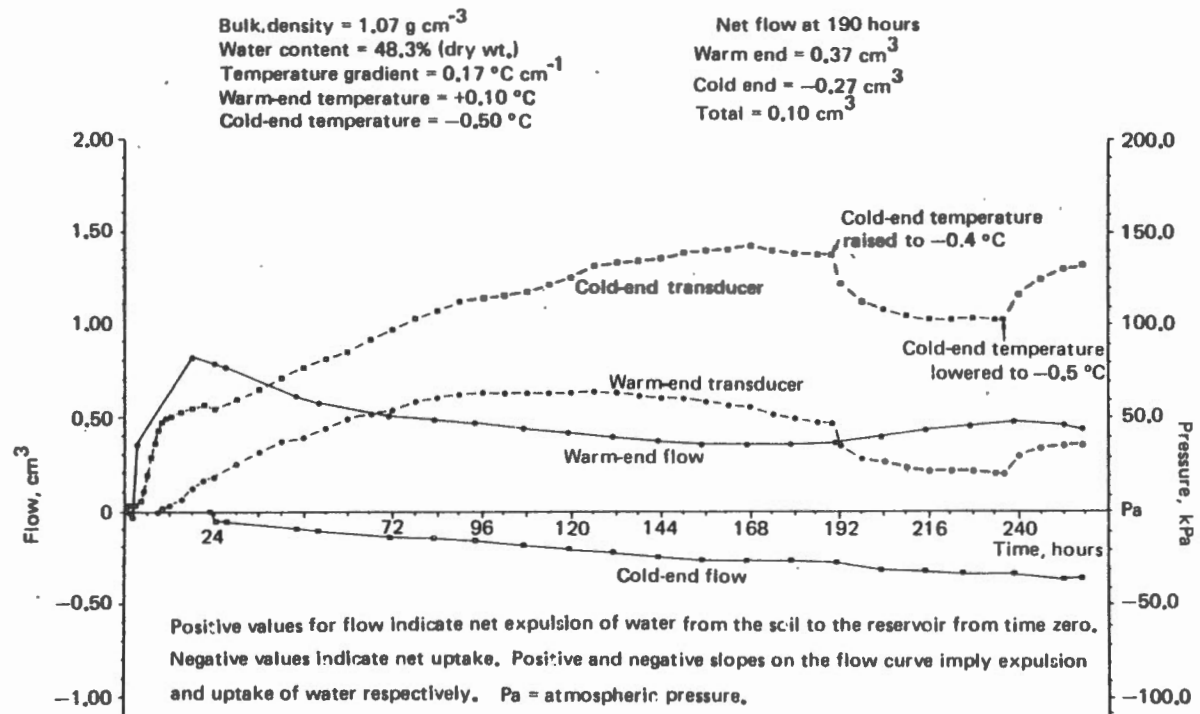


Figure 3.3
 Temperature Profile During Frost Heaving,
 Experiment 30, Allendale Clay

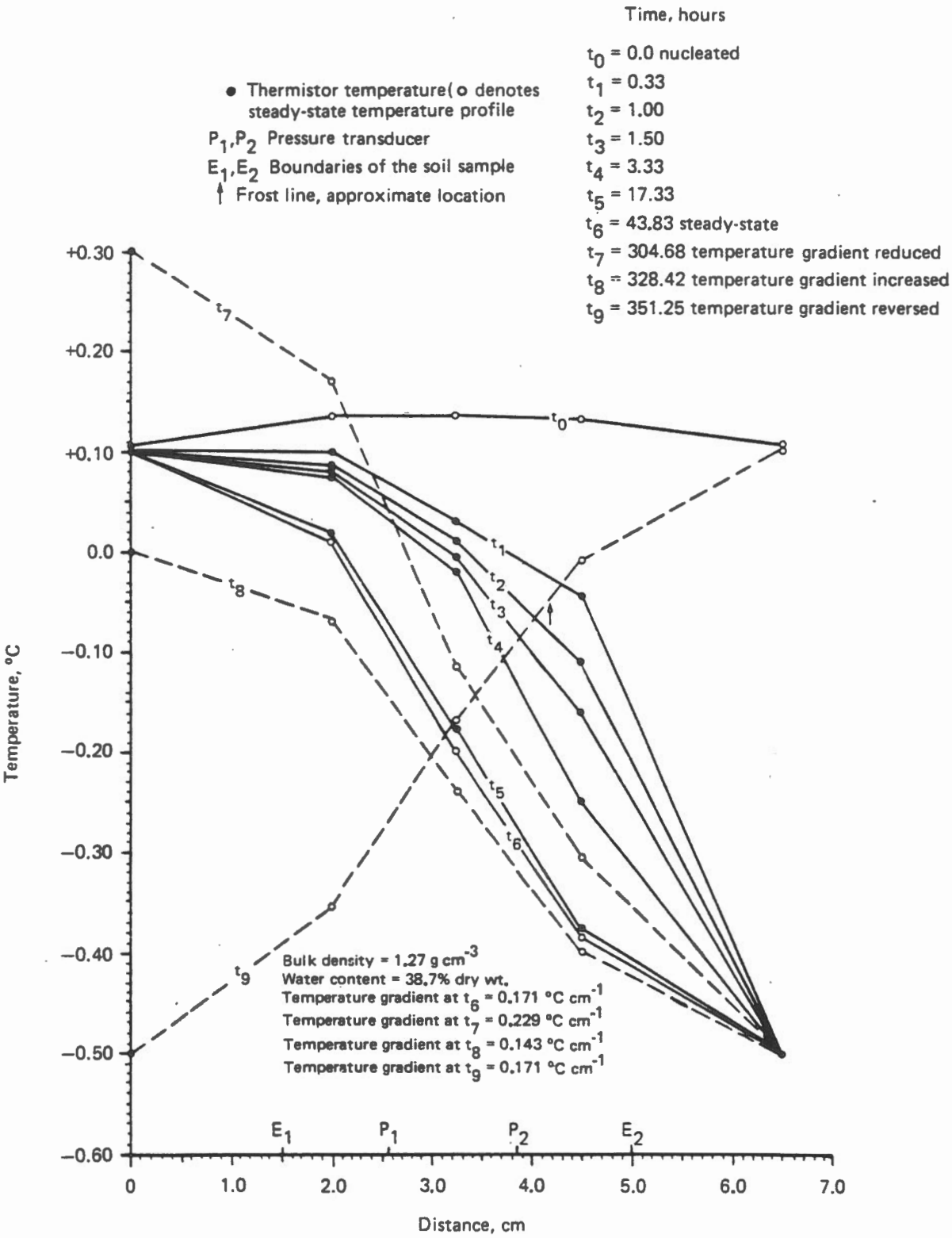


Figure 3.4
Flows and Internal Pressures During Frost Heaving, Experiment 30, Allendale Clay

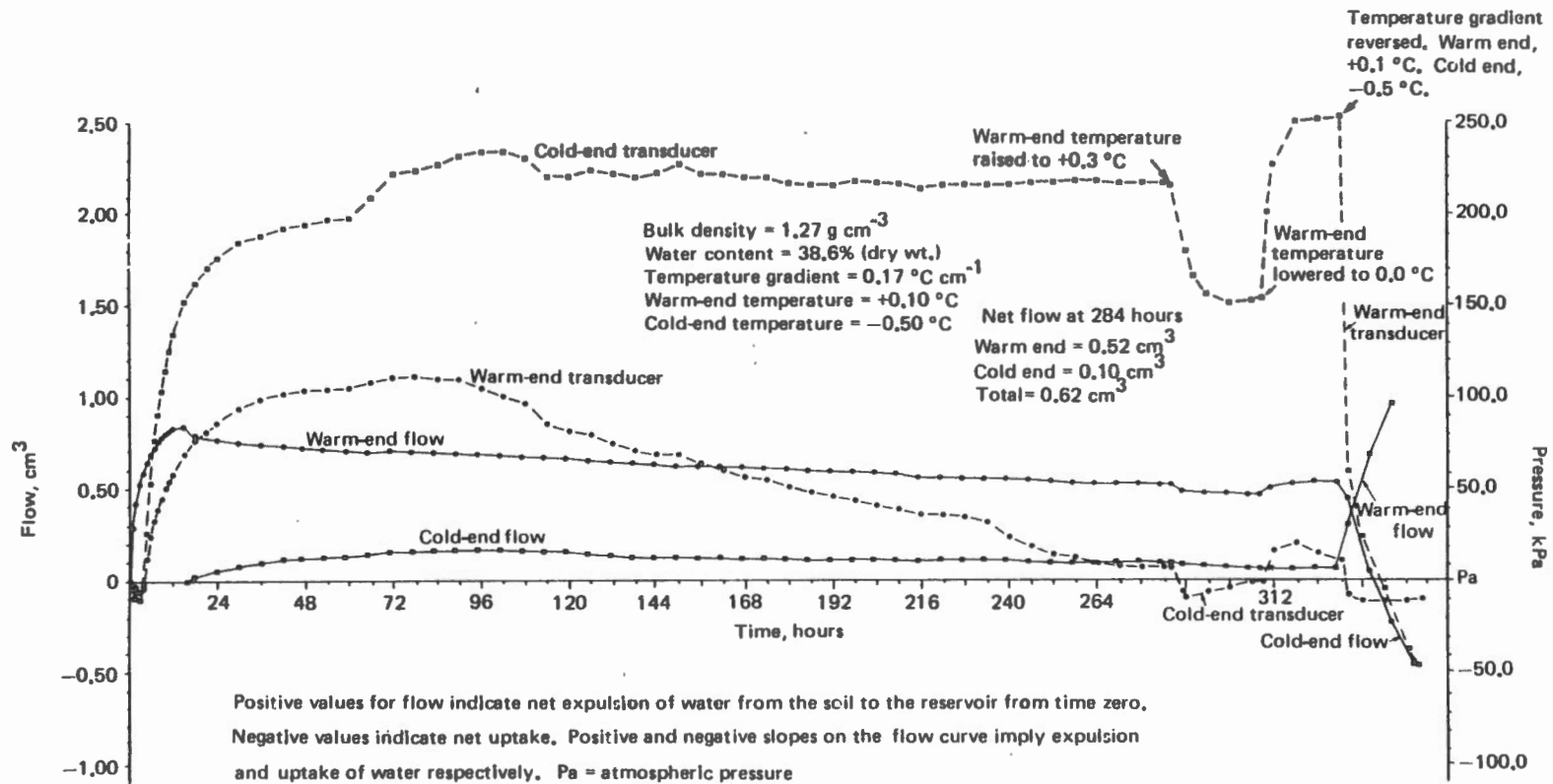


Figure 3.5
 Temperature Profile During Frost Heaving,
 Experiment 31, Caen Silt

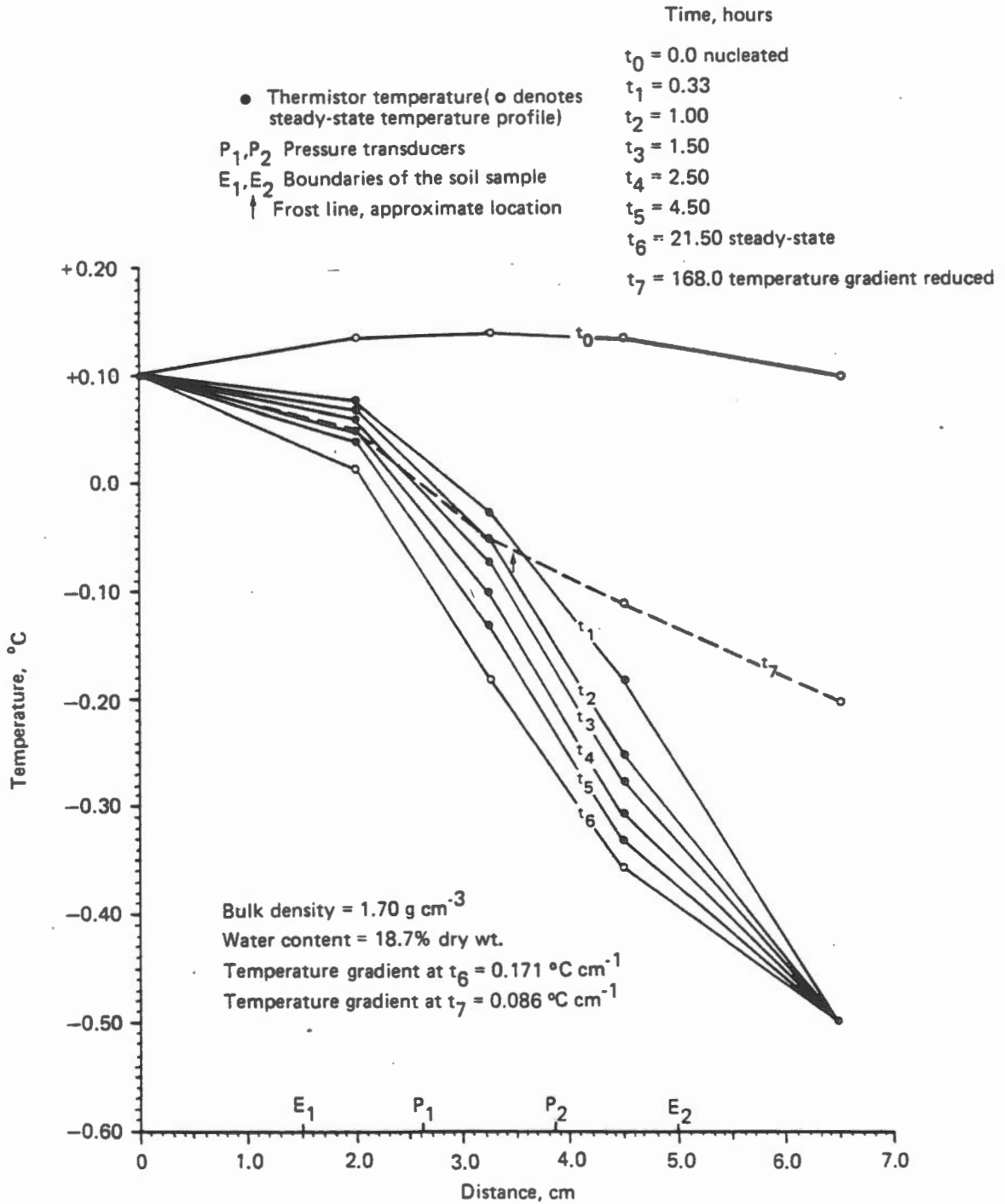


Figure 3.6
 Flows and Internal Pressures During Frost Heaving,
 Experiment 31, Caen Silt

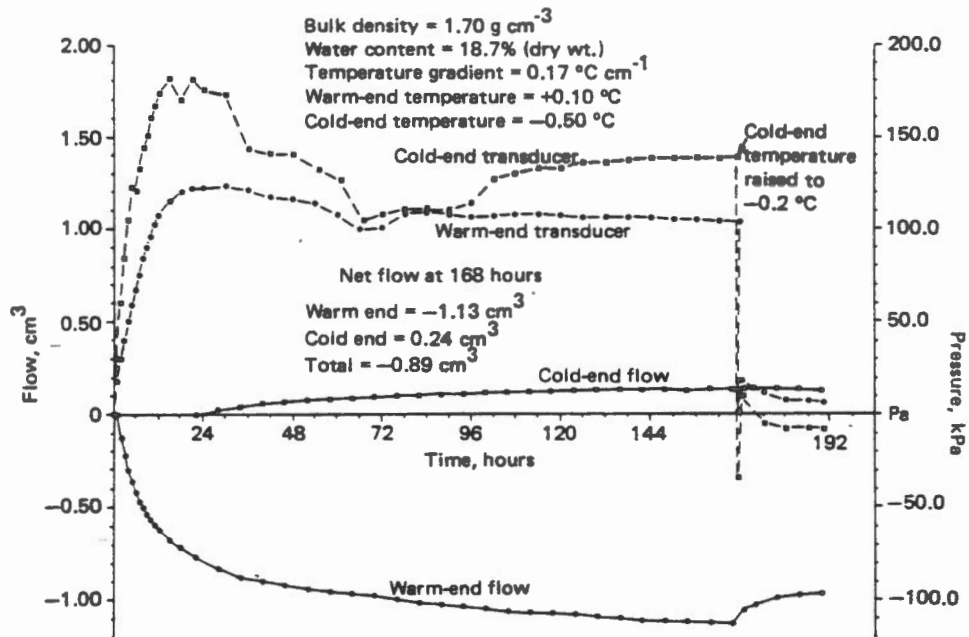


Figure 3.7
 Temperature Profile During Frost Heaving,
 Experiment 32A, Caen Silt

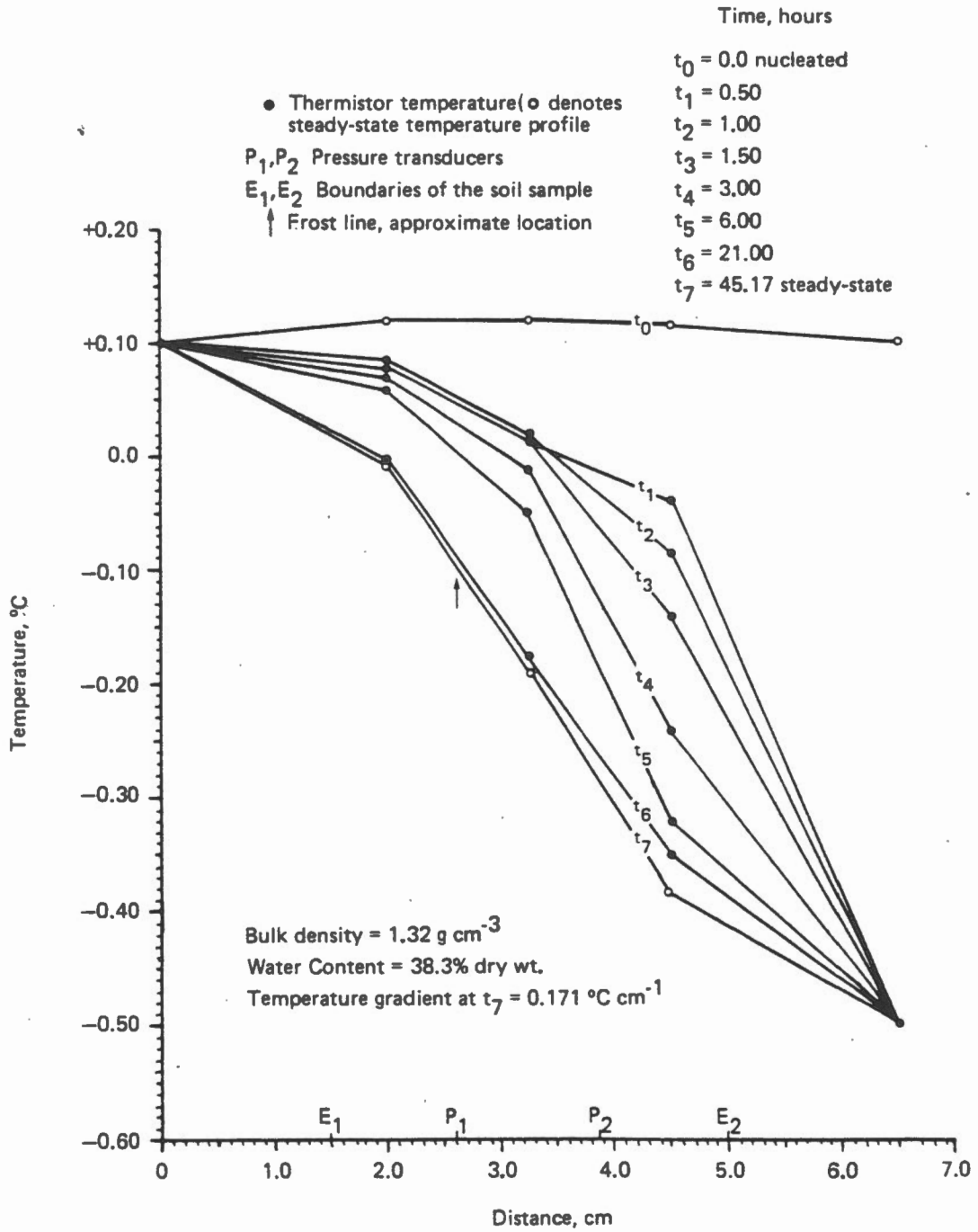
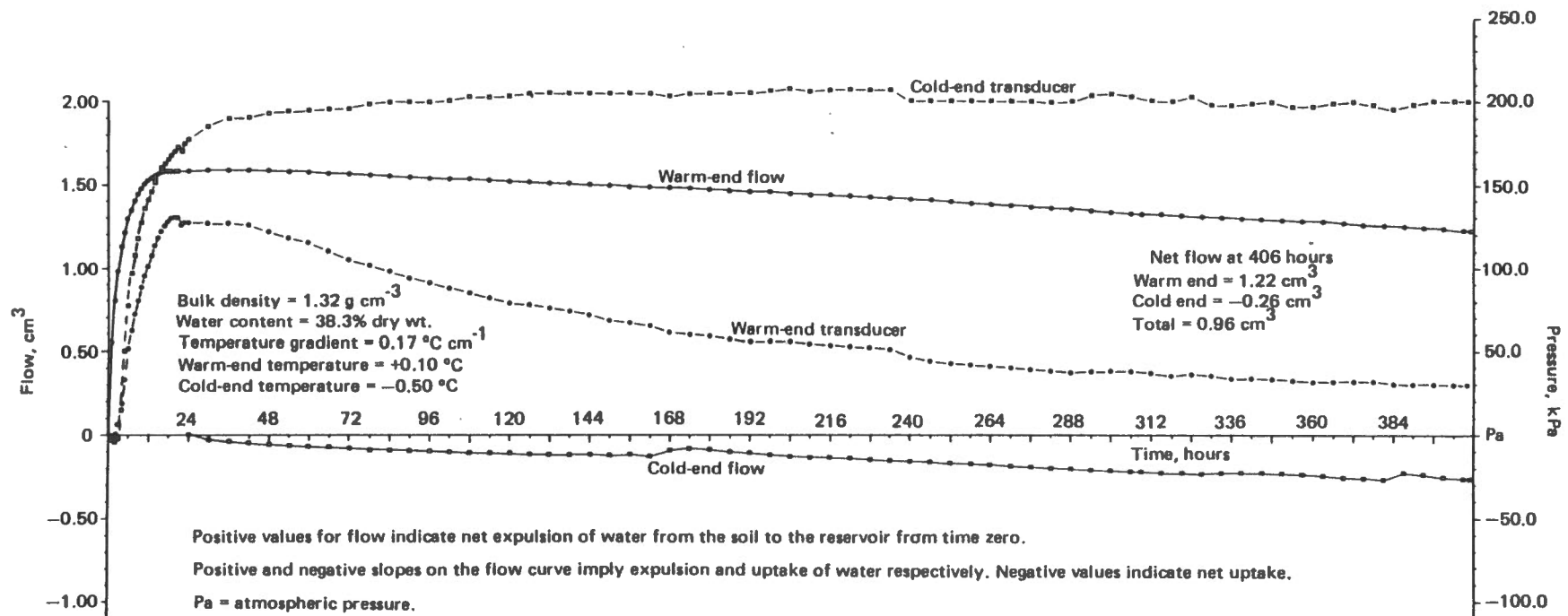


Figure 3.8
 Flows and Internal Pressures During Frost Heaving, Experiment 32A, Caen Silt



4. INTERPRETATION

4.1 Temperature and Heaving Pressure

The most interesting feature of the results is the very large difference in pressure between the warm and cold end transducers. This observation is accounted for by the Clausius-Clapeyron equation which relates changes in pressure to the temperature (Hillel, 1980):

$$V_w dP_w - V_i dP_i = \frac{LdT}{T}$$

where

P_i and P_w = the pressure of the ice and water, Nm^{-2}

$V_i = 1.091 \times 10^{-3} \text{ m}^3 \text{ kg}^{-1}$, specific volume of ice

$V_w = 1.000 \times 10^{-3} \text{ m}^3 \text{ kg}^{-1}$, specific volume of water

$L = 3.336 \times 10^5 \text{ J kg}^{-1}$, specific latent heat of fusion of
water

and $dT = T_o - T$ = difference between the normal freezing
temperature of pure water, $T_o = 273.15 \text{ K}$ and the
actual temperature, T of the system.

This equation explains the coexistence of ice and water in frozen soils as a result of a positive pressure in the ice phase and/or a suction in the liquid phase. If the water pressure is assumed to remain constant ($dP_w = 0$), the Clausius-Clapeyron equation predicts an increase in the ice pressure with decreasing temperature of 1.127 MPaK^{-1} (below normal freezing temperature). If $dP_i = 0$, the suction of the unfrozen water increases with lower temperatures by 1.229 MPaK^{-1} .¹

¹ The discrepancy in the magnitude of the pressure change between the two cases (0.102 MPaK^{-1}) arises as a result of the 9.1% difference in the specific volume of ice and water.

Early theories of frost heaving suggested that ice lenses form at the boundary between the frozen and unfrozen soil. However, it has recently been established that ice lenses actually start to form in the frozen soil a short distance behind the frost line (Miller, 1978). The frozen zone between the first ice lens and the frost line has been dubbed the 'frozen fringe' by Miller. Conditions within the fringe are critical to the growth of the lens. Contemporary theory suggests that, as the ice lens forms, the frost line advances and the frozen fringe becomes progressively thicker. Eventually an unstable condition is reached and a new ice lens begins to form just behind the frost line. While the new lens forms, older lenses continue to develop slowly as a result of continuous migration of water and ice toward colder regions in the frozen soil. The latter is usually referred to as 'secondary frost heaving'.

In the frozen fringe, the Clausius-Clapeyron equation is satisfied by the development of a suction within the unfrozen water. Water is drawn toward the lens along a suction gradient caused by temperature differences within the soil. At the base of the lens, a state of thermodynamic instability exists within the water, resulting in the excess water spontaneously changing to ice and accumulating as a layer, which pushes the adjacent soil layers apart. The Clausius-Clapeyron equation implies a theoretical upper limit of 1.127 MPaK^{-1} , for the pressure exerted by the ice lens on its surroundings, assuming $dP_w = 0$ and $P_w =$ atmospheric pressure at the base of the lens. Thus, the location of the lens with respect to the temperature of the soil is of crucial importance in determining the pressures that will develop.

4.2 Physical Manifestation of Frost Heave

When an ice lens forms, there is an increase in the entropy of the soil water, associated with freezing, implying a change to a state of greater stability (lower Gibbs potential). The first law of thermodynamics indicates that the enthalpy or expansive work done by the soil against its surroundings is achieved in either of two ways, (1) by increasing its volume while the pressure remains constant, or (2) by a build-up of pressure while the volume remains constant.

In practical situations, usually frost heaving is manifested as some combination of both of these changes. In the case of an unconfined soil where there is no resistance to expansion, as occurs near the soil surface, heaving is manifested largely as a volume change with unrestricted growth of ice lenses although, as discussed later in this report, there must be a build-up of internal pressure since the intervening layers of frozen soil between lenses provide some resistance to deformation. In the case where the soil is confined, as occurs in the present experiment (or under a large overburden), the work of frost heaving is achieved mainly as a rise in pressure, with little change in volume.² With our experiment, although the cell is essentially rigid, the soil itself is compressible, at least to a degree, and some ice lensing was apparent. The largest ice lenses observed were about 0.05 cm thick and concentrated in a zone near the cold end. These presumably developed simultaneously with some internal

² Although the concept of frost heaving, manifested as a rise in pressure without accompanying growth of ice lenses seems obvious, it has proven to be difficult for some researchers to grasp.

consolidation of the soil matrix in the unfrozen zone and possibly the frozen section as well. However, the volume change of the entire sample is probably miniscule since the cell has a very low bulk modulus (volume modulus of elasticity).

4.3 Role of Yield Stress in Determining Frost Heaving Pressures

It is well established that the strength of frozen soils is considerably greater than in the unfrozen state. The magnitude of the yield stress increases rapidly with lower temperatures and is also time dependent (Tsyrovich, 1975). In view of this, it would be expected that the intervening layers of frozen ground between ice lenses would provide resistance to the growth of ice lenses causing the pressure to build-up within each lens.³ Thus, the upper limit of pressure generated by each lens might be expected to be dependent upon the yield stress of the adjacent frozen material. Pressure is transmitted from each lens to the surroundings by yielding of the intervening frozen soil through creep. The implication of this is that, the fraction of the pressure generated by the lens, which is counteracted by the rigidity of the frozen soil matrix, would not be available as part of the externally effective frost heave pressure.

³ The exception to this would occur when the frozen soil is lifted in its entirety by an ice lens and undergoes a uniform linear displacement. Since the frozen soil above the lens is not directly bonded to that beneath it, there can be no resistance to displacement provided by the strength of the soil. This would only occur in a limited situation such as a frost heaving cell where an ice lens develops across the entire cross-sectional area of the sample and would not be expected under natural conditions since ice lenses are generally limited in areal extent.

In summary, we suggest that there are two types of pressure associated with frost heaving:

- (1) The internal pressure developed at the site of an ice lens, the upper limit of which is a direct function of the temperature, as specified by the Clausius-Clapeyron equation.
- (2) The externally effective frost heave pressure, which has a lower value owing to dissipation of the stress in the surrounding semi-rigid material.

The latter depends upon the creep and strength properties of the soil which have both a temperature and time-dependent nature. Thus, one would anticipate that, although the Clausius-Clapeyron equation predicts higher ice pressures at lower temperatures, the stresses would be transmitted less effectively to the surroundings owing to the increased strength of the frozen soil. In addition, the externally effective pressure might be expected to rise more slowly with time, as a result of creep of the frozen ground, which is temperature dependent.⁴

4.4 Significance of the Observed Pressure Difference

To address the question of why there is a difference in pressure between the warm and cold-end transducers, we suggest that a minute ice lens develops circumjacent to each rubber membrane displacing the oil and activating the transducer. This occurs because the oil is the

⁴ The long-term strength of a frozen soil is generally much lower than its instantaneous value, often by as much as an order of magnitude (Tsytovich, 1975).

weakest material in the system favouring yielding at this site. The pressures observed represent the pressure of the ice within each lens. As the frost line advances, the soil becomes colder and the ice pressure increases progressively. The maximum value is limited by the temperature at each transducer once a linear temperature gradient is established.

The pressure at the cold end is not established immediately after a thermal steady-state occurs but continues to rise for a number of days afterward owing to slow but continued creep of the frozen soil around the rubber membrane. Eventually the pressure stabilizes at a fairly constant peak value either due to, (1) yielding and consolidation of the soil during heaving, eventually reaching a maximum, or (2) a gradual increase in the strength of the frozen soil until it equals the stress generated by the ice lens, or (3) a combination of both of these changes.⁵

The thermal profile of the soil in experiments 30 and 32A indicates that the cold end transducer is located at the -0.285°C isotherm.⁶ The Clausius-Clapeyron equation indicates a theoretical maximum heaving pressure (assuming $dP_w = 0$ and $P_w =$ atmospheric pressure) of $1127 \text{ kPa } ^{\circ}\text{C}^{-1} \times 0.285^{\circ}\text{C} = 321 \text{ kPa}$ at this temperature which exceeds considerably the observed values (217 kPa in experiment

⁵ After the soil has cooled to stable temperatures, there may be continued growth of ice in the pores by a slow process of accretion until an equilibrium ice content is reached. In addition, bonds between the ice and the soil matrix may be strengthened further by recrystallization. Both of these changes would have the effect of increasing the yield stress of the material.

⁶ See t_7 , Figure 3.7.

30 and 200 kPa in experiment 32A). However, in both tests, the actual location of the frost line was determined to be approximately at the -0.080°C isotherm owing to the slight freezing-point depression produced by dissolved salts within the soil.⁷ Allowing for the fact that ice will not form in the soil until -0.080°C , the theoretical maximum ice pressure at the transducer decreases proportionally to $(-0.285^{\circ}\text{C} + 0.080^{\circ}\text{C}) \times 1127 \text{ kPa}^{\circ}\text{C}^{-1} = 231 \text{ kPa}$ which is very close to the observed values in both experiments (see Table 3.1).

In experiment 31, the pressure initially approached this value (171 kPa maximum) but then fell off sharply, apparently due to internal yielding within the soil. In the case of experiment 29, the pressure at the cold transducer only reached 143 kPa. This result can be attributed to the fact that the soil was not fully saturated during the preparations for the experiment, therefore some air was present in the soil pores.⁸ This has the effect of creating a counter-suction which restricts the flow of water toward the ice lens and limits the full development of heaving pressure.

⁷ With the Allendale soil, since the temperature gradient was reversed near the end of experiment 30, the frost line may not have reached a stable position by the time the cell was dismantled. Therefore, to avoid potential error, its position was assumed to be equal to that observed in experiment 29, where a steady-state prevailed. With the Caen soil, the value quoted above represents the mean of the observed values in experiments 31 and 32A.

⁸ Since experiment 29 was a preliminary trial to determine whether the apparatus was fully operational, the sample was prepared somewhat hastily without the attention to detail which was done in the other tests. Unfortunately, we neglected to de-air the soil in the vacuum chamber during the preparations and small bubbles were apparent throughout the sample. The volumetric water content of the soil was 51.7% and the actual volume fraction of pore space was 60.1%, implying 8.4% by volume filled with air. This undoubtedly had an effect on the results obtained.

Similarly, at the warm end, the pressure transducer is located approximately at the -0.095°C isotherm which is slightly behind the frost line, implying a heaving pressure of 22 kPa. In cases where the test was allowed to run long enough for the pressure to decline to a steady value, the observed pressures (7 kPa in experiment 30 and 30 kPa in experiment 32A) were found to be comparable to the theoretical maximum values. In the case of experiment 29, the temperature of the soil was changed before the pressure was allowed to stabilize and so the final value (48 kPa) was somewhat larger than the theoretical maximum.

4.5 Effect of Yielding

In experiment 31, large differences of 82 kPa at the warm end and -99 kPa at the cold end occurred between the observed pressures and the theoretical maximum values specified by the Clausius-Clapeyron equation, assuming $dP_w = 0$ (see Figure 3.6). This suggests that there was some form of internal yielding in the interjacent layer between the two transducers, dissipating the stresses generated by ice lenses at the cold end more uniformly throughout the soil. Thus, the pressure at the warm transducer would be higher than the predicted value and that at the cold end lower.

Yielding also accounts for the high pressures observed at the warm end at the start of each experiment, as well as the succeeding decline in pressure. Initially, during freezing, the strength of the soil is somewhat low owing to the fact that the soil has not attained its equilibrium ice content and ice-mineral bonds are not yet fully established. Thus, the high pressures at the warm transducer find their

origin in the colder regions of the soil. However, as the soil temperature decrease, the yield stress of the soil rises enabling higher stress gradients to be sustained and the pressure at the warm transducer declines to a value approaching that indicated by the Clausius-Clapeyron equation.

4.6 Explanation for Water Expulsion and Positive Soil Pressures

A seemingly contradictory result is the establishment of high pressures within the cell, while at the same time the soil experienced a net loss of water, chiefly by discharge from the warm end. However, this should not seem so surprising if one allows for the volume expansion of water during freezing. Assuming that the initial discharge of water represents the 9.1% volume increase when the water in the soil changes to ice, the total volume of water frozen is $0.84 \text{ cm}^3 \times \frac{100}{9.1} = 9.23 \text{ cm}^3$ in experiments 29 and 30 and 17.47 cm^3 in experiment 32A (see Table 4.1). This implies freezing of 22.3% and 23.4% of the pore fluid volume in experiments 29 and 30 and 43.1% in experiment 32A. The lower values for the Allendale clay are explained primarily by the colloidal nature of the soil, as opposed to the Caen soil which is composed mainly of silt.

The actual fraction of water turned to ice within the soil is probably somewhat higher than the values indicated above. The reason for this is that, if all the 9.1% volume increase associated with phase change is manifested as expulsion of water, the soil pressure would not rise. In reality, the total amount expelled must be somewhat lower than this value in order for pressure to be developed within the cell.

TABLE 4.1
Freezing Data, Experiments 29, 30 and 32A

Experiment Soil	29 Allendale	30 Allendale	32A Caen
Q_e	0.84	0.84	1.59
V_f	9.23	9.23	17.47
V_T	41.44	39.36	40.56
N_i	22.3	23.4	43.1

Q_e = volume of water expelled from the soil at the start of the experiment, cm^3

$V_f = Q_e \times \frac{100}{9.1}$ volume of water changed to ice in the soil, cm^3

$V_T = \theta \times V$ total volume of water within the soil, cm^3
(θ = volumetric water content of soil %. V = 80.16 cm^3 , volume of the cell)

$N_i = \frac{V_f}{V_T} \times 100$ volume fraction of pore fluid changed to ice, %

The expulsion of water from the warm end occurred during the initial 24 hours of the test when the frost line was still advancing through the soil. The discharge implies consolidation of the unfrozen soil caused by the growth of ice lenses near the cold end. Eventually, however, consolidation reaches a maximum and the soil can be compressed no further. At this point, the flow reverses and water is drawn into the soil at the warm end. Further development of ice lenses is manifested as a pressure increase rather than a volume change.

The uptake of water at the warm end continues at a slow but declining rate, even after the pressure at the cold end has levelled off, presumably because of continuous slow yielding (consolidation) of the frozen soil. Any tendency for the pressure to decline as a result of yielding is counteracted by the continued enlargement of ice lenses, so that a stable value is maintained. Eventually, however, the soil must reach a stage where no further yielding is possible and the uptake of water would presumably level off.

A puzzling feature of the results is why the soil appears to draw in water at the cold end in some tests and not in others. At the present time, there is no obvious explanation for this except that perhaps, the uptake is due to thawing at the cold end as a result of lactose diffusion into the soil. To determine the effects of thawing, in future, some tests will be run in which the sample is sealed off at the cold end by an impermeable barrier, allowing water access only at the warm end.

4.7 Significance of Soil Compressibility

A curious feature of the results is why there was such a large uptake of water in experiment 31 instead of the initial expulsion which was observed in the other tests. The obvious reason for this is that the soil was compacted to a very high density. We suggest that because the soil is practically incompressible, ice lenses are unable to form and the uptake of water during heaving is manifested almost entirely as a pressure increase rather than a volume change. Indeed, upon dismantling the cell, no ice lenses of even hairline thickness were observed.

In the other tests, the initial expulsion of water is due to the growth of ice lenses causing consolidation in the adjacent unfrozen zone and the expulsion of water. The water expelled primarily represents the 9.1% volume increase associated with the phase change from water to ice.

4.8 Effect of Temperature Gradient Changes on Internal Pressure

Raising and lowering the temperature of the cooling plate resulted in a fairly consistent pressure change of about 35 kPa for every 0.1°C. However, examining the results more closely reveals several important discrepancies (Table 4.2).

In all of the tests, the observed change in pressure at each transducer was always less than the change predicted by the Clausius-Clapeyron equation (ΔP_p in Table 4.2). For example, in experiment 29, at 190 hours, the temperature at the cold end was increased from -0.50°C to -0.40°C. The pressure decreased by 64 kPa at the cold end

TABLE 4.2

Pressure and Flow Changes Accompanying Changes
to the Pressure Gradient, Experiments 29-31

Experiment Soil	29 Allendale	29	30 Allendale	30	30	31 Caen
t	190	236	284	309	331	167.5
ΔT_{cp}	+0.10c	-0.10c	+0.20w	-0.30w	+0.60c/ -0.60w ^R	+0.30c
Cold end						
ΔT	+0.085	-0.085	+0.085	-0.110	+0.215	+0.185
ΔP_o	-36	+31	-64	+99	-297	-144
ΔP_p	-96	+96	-96	+124	-242	-203
Q	-0.056	-0.027	-0.029	-0.003	> -0.090	-0.008
Warm end						
ΔT	+0.050	-0.050	+0.120	-0.175	-0.100	+0.080
ΔP_o	-27	+15	-7	+12	-22	-95
ΔP_p	-34*	+34*	-22*	+85*	+113	-6*
Q	+0.090	-0.021	-0.051	+0.069	> +0.090	+0.260

t time temperature change was initiated, hrs (see Figures 3.1-3.8)

ΔT_{cp} temperature change at the cooling plate, °C. c and w denote changes in the temperature of the cold and warm plates respectively. R denotes reversal of the temperature gradient. (Positive values indicate an increase in the temperature and negative values, a decrease.)

ΔT temperature change at the pressure transducer, °C

... continued

TABLE 4.2 (continued)

ΔP_o	observed pressure change, kPa. (Positive values indicate an increase in pressure and negative values a decrease.)
$\Delta P_p =$	$\Delta T \times 1127 \text{ kPa } ^\circ\text{C}^{-1}$ pressure change indicated by the Clausius-Clapeyron equation, assuming $dP_w = 0$ and $P_w =$ atmospheric pressure. * signifies that the temperature at the transducer surpassed the natural freezing-point depression of the soil. Ideally, at above freezing temperatures, the soil pressure cannot change further and should stabilize at atmospheric pressure.)
Q	flow to/from the soil accompanying temperature change, cm^3 . (Positive values indicate outflow and negative values, uptake of water.)

and 27 kPa at the warm end. The decreases predicted by the Clausius-Clapeyron equation (assuming $dP_w = 0$) were 96 kPa and 34 kPa respectively. Similarly, when the cold end was lowered again to -0.50°C at 236 hours, the pressure increased by 31 kPa at the cold transducer and 15 kPa at the warm transducer which is also less than the increases predicted by the Clausius-Clapeyron equation (see Table 4.2).

The most likely explanation for these differences is that there is a considerable lag between the temperature change at each transducer and the establishment of stable pressures. In other words, if sufficient time had been allowed, the observed pressure change would have eventually reached a value close to the predicted change. Careful examination of the pressure and flow diagrams (Figures 3.2, 3.4 and 3.6) reveals that the pressures had not stabilized completely, even two days after the temperature change, and still continued to increase or decrease very slowly, suggesting that this explanation is true.

In a number of cases, temperature changes caused the frost line to advance past the transducer (indicated by an * in Table 4.2), implying complete thawing (or freezing) of the soil around the transducer. In most instances, thawing of the soil resulted in a corresponding decline in the pressure at the transducer to subatmospheric values (examples: experiment 30 at 331 hours and experiment 31 at 167.5 hours). This occurs because the 9.1% volume decrease due to thawing of ice within the soil cannot be balanced rapidly enough by the influx of water (owing to the low permeability of the soil) and so a state of suction is temporarily established.

Near the end of experiment 30, the temperature gradient was reversed (Figure 3.4). The pressure at the warm end* (formerly the cold end) declined sharply to about 50 kPa below atmospheric pressure as a result of thawing of ice at this location.⁹ At the cold end* (formerly the warm end), the pressure declined to about 10 kPa below atmospheric pressure and did not show any tendency to increase as was expected. One possible explanation for this is that insufficient time was allowed for the redistribution of water and ice within the soil and that ultimately, the pressure would have risen. There is also a possibility that ice was prevented from forming further by diffusion of lactose into the soil during the temperature change.¹⁰

Contrary to expectations, there was a large uptake of water by the cold end* of the soil and expulsion by the warm end*. At the warm end*, the decrease in volume associated with thawing of ice within the soil should result in the uptake of water. In contrast, at the cold end* volume increases associated with freezing should cause expulsion. A suggested explanation for the observed result is that the strong suction gradients established by freezing at the cold end* cause water to be drawn into the soil, from the reservoir, toward the frost line.

⁹ * signifies the temperature at the boundaries of the soil after the thermal gradient was reversed, i.e. warm end* (formerly the cold end) or cold end* (formerly the warm end).

¹⁰ As mentioned earlier, a small thawed zone was observed at the cold end of the soil at the end of each experiment, implying the slow diffusion of lactose molecules into the soil. If the temperature gradient is reversed, at the warm end* (formerly the cold end) lactose might diffuse rapidly through the soil and could have a significant effect on the results. It is proposed that, in future tests involving reversal of the temperature gradient, the use of lactose will be avoided.

Volume increases associated with freezing result in consolidation and expulsion at the warm end* where the strength of the soil is diminishing as it warms up.

4.9 Measurement of Externally Effective Frost Heaving Pressure

As mentioned earlier, the pressures developed at each transducer represent the internal pressure of an ice lens at that specific location within the soil thermal profile. Although the present set-up does not allow direct measurement of the externally effective frost heaving pressure, we believe that this could be accomplished rather easily with a few simple modifications to the cell. These would involve connecting the cold reservoir to a pressure transducer and removing the porous aluminum disc which supports the semi-permeable membrane. If the reservoir is filled with a non-freezing fluid (mercury) and an impermeable rubber membrane fitted over the cold end of the soil, the pressure measured would be that of the entire soil sample.

4.10 Concluding Remarks

Although in retrospect our rationale might seem obvious, to our knowledge, the idea of the strength of the soil limiting the heaving pressure has not been considered previously. It is tacitly assumed in current frost heaving theory, that the internal pressure is uniform in frozen soils and it is transmitted unimpeded to the surroundings.

Finally, although frost heaving has not been considered from this point of view, there are a number of references in the literature which

corroborate our experimental findings. Observations of pressure differences up to 60 kPa over 0.5 m in seasonally frozen ground are noted by Tsytoovich (1975). Mackay (1983) also recorded, over a period of several months, fluctuating positive pressure differences up to 110 kPa over 0.5 m in the field using small pressure cells at depths down to 1 metre. This greatly exceeds the overburden pressure suggesting that the strength of the frozen soil effectively acts as an overburden. Similarly at the Canada-France ground-pipeline freezing project in Caen, France, observations from Glotzl cells buried at depths down to 1 metre below the pipe have shown pressure differences up to 60 kPa over 0.35 m, within the annulus of frozen ground around the pipe (Guichaoua and Williams, 1984).

SUMMARY

1. An especially designed cell allows measurement of internal frost heaving pressures in frozen soils. Results indicate that during freezing, the internal stresses are not uniform. Instead, it appears that the soil is able to sustain high pressure gradients, the pressure generally increasing with colder temperatures. Pressure gradients of up to 200 kPa cm^{-1} have been measured.

2. We suggest that the creep and strength properties of frozen soils play an integral role in determining the effective frost heaving pressure. In practical terms, the heaving pressure exerted by a growing ice lens is limited by the strength of the circumjacent frozen material. The greater the strength of the soil, the higher the stress gradient sustained around each lens. Thus, one can speak of two types of pressure associated with frost heaving:
 - (i) The internal pressure developed within an ice lens which has a theoretical maximum value controlled by the temperature.
 - (ii) The externally effective pressure which has a somewhat lower value owing to dissipation of the stress in the surrounding frozen material.

The externally effective pressure represents the difference between the internal pressure generated at the site of the ice lens and the long-term yield stress of the intervening frozen soil.

3. The frost heaving cell is designed with two miniature pressure transducer assemblies, each of which is attached to a very small rubber membrane filled with oil, which is located within the soil and acts as the pressure sensitive medium. We suggest that, since the oil is the weakest material in the system, a tiny ice lens forms around each membrane during freezing. Thus, the pressure measured by each transducer represents the internal pressure of an ice lens at that particular temperature.
4. The Clausius-Clapeyron equation predicts a theoretical maximum ice pressure of 1.127 MPa for every degree Kelvin below freezing, assuming the water pressure remains constant at atmospheric pressure. In practice, this value is never fully attained owing to creep of the intervening frozen soil between the two transducers. Yielding results in a tendency toward a more uniform distribution of stress within the soil. Thus, the pressure at the cold end tends to be slightly less than its predicted value and that at the warm end somewhat greater.
5. In the early stages of freezing, the pressure gradients within the frozen zone are generally much smaller. This occurs because the strength of the soil is not yet fully established. However, as the soil temperature declines, the yield stress increases resulting in an increase in the pressure gradient toward a final stable value, which is determined by the long-term yield stress of the soil.

6. In the case of an unconfined soil, the tendency toward a more uniform stress distribution during freezing would be greater owing to the potential for unlimited and unrestrained yielding of the soil. However, in a confined soil, ultimately the ice pressure would approach its theoretical maximum value since yielding of the soil is limited by the confining stress.

REFERENCES

- Hillel, D. 1980 'Applications of Soil Physics'. Academic Press, New York, p. 259.
- Mackay J.R. 1983 'Downward Water Movement Into Frozen Ground, Western Arctic Coast, Canada'. Canadian Journal of Earth Science, p. 120-134.
- Miller R.D. 1978 'Frost Heaving in Non-Colloidal Soils'. Proceedings of the Third International Conference on Permafrost, Edmonton Alberta, V. 1, p. 708-713.
- Tsyтович N.A. 1975 'The Mechanics of Frozen Ground'. McGraw-Hill, 426 p.
- Torrance J.K. and Wood J.A. 1983 'Investigation of Temperature-Induced Stresses and Water Movements in Frozen Soils'. Final Report to the Department of Energy Mines and Resources, Ottawa, Canada, DSS File No 24SU 23235-2-0581.
- Guichaoua A and Williams P.J. 1984 'Expérimentation sur La Gel d'un Sol Et D'une Canalisation Enterrée Et Refroidie Dans Une Installation D'essai De Grandes Dimensions'. Third Phase. Final Report to the Department of Energy Mines and Resources, Ottawa, Canada, DSS File 03SU 23235-3-1059, p. 20-21.

APPENDIX A
CALIBRATION REPORTS FOR PRESSURE TRANSDUCERS



KULITE

SEMICONDUCTOR



PRESSURE TRANSDUCER TEST REPORT

MODEL NO. VQS-250-50 SG

SERIAL NO. 4505-5-76

CUSTOMER DURHAM

CUSTOMER P.O. No. R831401

STANDARD ELECTRICAL CONNECTIONS: (Per ISA 37.1)

SPECIAL CONNECTIONS:

Red - + Input
 Black - - Input

Green - + Output
 White - - Output

TEST CONDITIONS:

Rated Pressure 50 psi SG

 Gage X Sealed Gage

Maximum Pressure 100 psi SG

Maximum Reference Pressure psi

 Absolute Differential

Tested at 5 VDC Excitation

Maximum Excitation: 7.5 VDC

SPECIFICATIONS:

Sensitivity: .902 mV/psi

Zero Pressure Output: < +3% F.S.

Thermal Effect on Zero: < +1 % FS/100°F Not Compensated

Thermal Effect on Sensitivity: < +2 %/100°F Not Compensated*

Compensated Temperature Range: 14°F to 86°F (-10°C to 30°C)

Output Impedance 364 ohms Input Impedance 732 ohms

*See Bulletin for external compensation method.

REMARKS:

SILASTIC COATING ON DIAPHRAGM. O-RING SUPPLIED.

UNIT PARYLENE-COATED.

NEW TEST REPORT BEING ISSUED AFTER REPLACEMENT OF COMPENSATION

MODULE.

QUALITY ASSURANCE:

Tested by H. S.

Inspected by  A47

Date AUG 10 1983

Date AUG 10 1983

KULITE SEMICONDUCTOR PRODUCTS, INC. • 1039 Hoyt Avenue • Ridgefield, New Jersey 07657 • Tel: 201-945-3000 • Cable: Kultung • Telex: 135 458

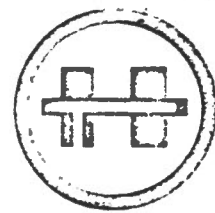
UNITED KINGDOM • KULITE SENSORS LTD
 P.O. Box 28 • Aachen Lane
 Basingstoke, Hants RG21 1AF England
 Tel: 0256 65467 • Telex: 851-858-434 (BB) KULITE G

GERMANY • KULITE SEMICONDUCTOR PRODUCTS GmbH
 Postfach 1527 6236 Hofheim-Ts West Germany
 Tel: (49) 06192 39050 • Telex: 841-416-016 (00) KULIT D

FRANCE • J.P.B.
 Distributors for KULITE INTERNATIONAL S.A.R.L.
 11 Rue Laperouse 76390 • Bois-D'Arcy France
 Tel: (3) 460 13 55 • Telex: 695 626 F



KULITE SEMICONDUCTOR



PRESSURE TRANSDUCER TEST REPORT

MODEL NO. VQS-250-50 SG

SERIAL NO. 1025-7-126

CUSTOMER DURHAM

CUSTOMER P.O. No. R831401

STANDARD ELECTRICAL CONNECTIONS: (Per ISA 37.1)

SPECIAL CONNECTIONS:

Red - + Input
Black - - Input

Green - + Output
White - - Output

TEST CONDITIONS:

Rated Pressure 50 psi SG

 Gage X Sealed Gage

Maximum Pressure 100 psi SG

Maximum Reference Pressure psi

 Absolute Differential

Tested at 5 VDC Excitation

Maximum Excitation: 7.5 VDC

SPECIFICATIONS:

Sensitivity: .902 mV/psi

Zero Pressure Output: < +3% F.S.

Thermal Effect on Zero: < +1 % FS/100°F

 Not Compensated

Thermal Effect on Sensitivity: < +2 %/100°F

 Not Compensated*

Compensated Temperature Range: 14°F to 86°F (-10°C to 30°C)

Output Impedance 359 ohms

Input Impedance 646 ohms

*See Bulletin for external compensation method.

REMARKS:

SILASTIC COATING ON DIAPHRAGM. O-RING SUPPLIED.

UNIT PARYLENE-COATED.

REPLACEMENT FOR S. N. 4417-2-19

QUALITY ASSURANCE:

Tested by H. S.

Inspected by



Date SEP 30 1983

Date OCT 4 1983

KULITE SEMICONDUCTOR PRODUCTS, INC. • 1039 Hoyt Avenue • Ridgefield, New Jersey 07657 • Tel: 201-945-3000 • Cable: Kultung • Telex: 135 458

UNITED KINGDOM • KULITE SENSORS LTD
P.O. Box 26 • Alencon Link
Basingstoke Hants RG21 1AF England
Tel: 0256 61646 7 • Telex: 851-858-434-BB: KULITE G

GERMANY • KULITE SEMICONDUCTOR PRODUCTS GmbH
Postfach 1527 6238 Hofheim/Ts West Germany
Tel: 049-06192 39090 • Telex: 841-416-016-00: KULIT D

FRANCE • J.P.B
Distributors for KULITE INTERNATIONAL S.A.R.L.
11 Rue Lacerousse 78390 • Boissery France
Tel: 031460 13 55 • Telex: 695 625 F



BUCHAN INSTRUMENTS
division of BUCHAN INSTRUMENTS INC.

P.O. BOX 426 PICKERING, ONT. L1V 2R7 • TELEX: 06-981474
TORONTO (416) 839-9960 • OTTAWA (613) 238-4200
MONTREAL (514) 286-9797 • VANCOUVER (604) 278-7755

PRESSURE TRANSDUCER TEST REPORT

MODEL NO. VQS-250-50 SG SERIAL NO. 1025-7-106
CUSTOMER DURHAM CUSTOMER P.O. R831689

STANDARD ELECTRICAL CONNECTIONS: (Per ISA 37.1)

Red — +Input Green — +Output
Black — -Input White — -Output

SPECIAL CONNECTIONS:

TEST CONDITIONS:

Rated Pressure 50 psi SG Gage X Sealed Gage
Maximum Pressure 100 psi SG
Maximum Reference Pressure psi Absolute Differential
Tested at 5 VDC Excitation Maximum Excitation: 7.5 VDC

SPECIFICATIONS:

Sensitivity: .897 mV/psi
Zero Pressure Output: < ± 3% F.S.
Thermal Effect on Zero: < +1 %FS/100°F Not Compensated
Thermal Effect on Sensitivity: < +2 %/100°F Not Compensated*
Compensated Temperature Range: 14°F to 86°F (-10°C to +30°C)
Output Impedance 352 ohms Input Impedance 668 ohms

*See Bulletin for external compensation method.

REMARKS: O-Ring Supplied Copper Washer Supplied
 "M" Screen Added "B" Screen Added

UNIT PARYLENE-COATED.
SILASTIC COATING ON DIAPHRAGM.
REPLACEMENT FOR S. N. 4505-5-81

QUALITY ASSURANCE:

TESTED BY H. S.

INSPECTED BY 

DATE 12-13-83

DATE DEC 14 1983

PRESSURE TRANSDUCER TEST REPORT

MODEL NO. VQS-250-50 SG SERIAL NO. 1025-7-73
 CUSTOMER DURHAM CUSTOMER P.O. R831689

STANDARD ELECTRICAL CONNECTIONS: (Per ISA 37.1)

Red — +Input Green — +Output
 Black — -Input White — -Output

SPECIAL CONNECTIONS:

TEST CONDITIONS:

Rated Pressure 50 psi SG _____ Gage X Sealed Gage
 Maximum Pressure 100 psi SG
 Maximum Reference Pressure _____ psi _____ Absolute _____ Differential
 Tested at 5 VDC Excitation Maximum Excitation: 7.5 VDC

SPECIFICATIONS:

Sensitivity: .889 mV/psi
 Zero Pressure Output: < ± 3% F.S.
 Thermal Effect on Zero: < +1 %FS/100°F _____ Not Compensated
 Thermal Effect on Sensitivity: < +2 %/100°F _____ Not Compensated*
 Compensated Temperature Range: 14°F to 86°F (-10°C to +30°C)
 Output Impedance 362 ohms Input Impedance 649 ohms
 *See Bulletin _____ for external compensation method.

REMARKS: O-Ring Supplied Copper Washer Supplied
 "M" Screen Added "B" Screen Added

UNIT PARYLENE-COATED.
 SILASTIC COATING ON DIAPHRAGM.
 REPLACEMENT FOR S. N. 4505-5-79

QUALITY ASSURANCE:

TESTED BY H. S.

INSPECTED BY  A47

DATE 12-13-83

DATE DEC 14 1983



KULITE SEMICONDUCTOR



PRESSURE TRANSDUCER TEST REPORT

(ORDERED AS XTM-1-190-100 SG)

MODEL NO. XTM-190-100 SG NEW MODEL

SERIAL NO. 375-5-114 (R4-40)

CUSTOMER DURHAM

CUSTOMER P.O. No. 1890

STANDARD ELECTRICAL CONNECTIONS: (Per ISA 37.1)

Red - + Input
Black - - Input

Green - + Output
White - - Output

SPECIAL CONNECTIONS:

TEST CONDITIONS:

Rated Pressure 100 psi SG

 Gage X Sealed Gage

Maximum Pressure 200 psi SG

Maximum Reference Pressure psi

 Absolute Differential

Tested at 5 VDC Excitation

Maximum Excitation: 7.5 VDC

SPECIFICATIONS:

Sensitivity: .403 mV/psi

Zero Pressure Output: < +3% F.S.

Thermal Effect on Zero: < +2 % FS/100°F Not Compensated

Thermal Effect on Sensitivity: < +2 %/100°F Not Compensated*

Compensated Temperature Range: 14°F to 86°F (-10°C to +30°C)

Output Impedance 328 ohms Input Impedance 965 ohms

*See Bulletin for external compensation method.

REMARKS:

O-RING SUPPLIED.

MAXIMUM TORQUE 15 INCH POUNDS.

QUALITY ASSURANCE:



Tested by M. S.

Inspected by

Date 12-29-81

Date DEC 29 1981

APPENDIX B

DESIGN SPECIFICATIONS OF FROST HEAVING CELL

1. Plexiglass sample container
 - Inner diameter 5.39 cm
 - Inner length 3.55 cm
 - Wall thickness 3.41 cm

2. Aluminum cooling plates
 - Overall thickness 1.78 cm
 - Outer flange diameter 8.12 cm
 - Outer flange thickness 0.83 cm
 - Inner flange diameter 6.75 cm
 - Inner flange thickness 0.62 cm
 - (i) O-ring outer diameter 7.00 cm
 - O-ring thickness 0.36 cm
 - O-ring flange diameter 6.35 cm
 - O-ring flange thickness 0.32 cm
 - (ii) Reservoir diameter 5.40 cm
 - Reservoir thickness 0.17 cm
 - Feed through gland diameter 0.20 cm

3. Porous aluminum plates (membrane supports)
 - Thickness 0.62 cm
 - Diameter 6.03 cm
 - Holes 0.20 cm diameter drilled vertically 0.25 cm apart
 - (i) Wire mesh diameter 5.50 cm
 - Wire mesh thickness 0.03 cm

4. Brass heat sinks
 - Diameter 6.30 cm
 - Thickness 1.05 cm

5. Peltier modules (15 amp 120 V.d.c.)
 - Length 3.00 cm
 - Thickness 0.45 cm

6. Pressure Transducers (Kulite VQS-250 series)
 - Length 1.72 cm
 - Inner diameter 0.64 cm
 - Outer (flange) diameter 0.78 cm
 - (i) O-ring outer diameter 0.95 cm
 - O-ring thickness 0.18 cm
 - (ii) Copper tubes
 - Length 1.55 cm
 - Outer diameter 0.31 cm
 - Inner diameter 0.21 cm
 - Flange diameter 0.62 cm
 - (iia) O-ring outer diameter 0.95 cm
 - O-ring thickness 0.18 cm
 - (iii) Adjustable brass sleeve (adjusted by turning a small screw)
 - Diameter (approx.) 0.53 cm
 - Width 0.50 cm

- (iv) Plexiglass retaining nuts
 - Length 0.90 cm
 - Outer thread diameter 0.89 cm
 - Thickness of head 0.19 cm
- (iva) Plexiglass extension tubes
 - Length 1.90 cm
 - Outer diameter 0.65 cm
 - Inner diameter 0.33 cm

7. Thermistors (YSI 3000 Ω)

- (i) Copper housing tubes
 - Length 2.45 cm
 - Outer diameter 0.31 cm
 - Inner diameter 0.21 cm
 - Flange diameter 0.60 cm
- (ii) O-ring outer diameter 0.95 cm
- O-ring thickness 0.18 cm

APPENDIX C

LIST OF EQUIPMENT USED IN THE EXPERIMENT

1. Precision low temperature incubator, model 815
2. Hotpack refrigerated bath circulator, model 603340
3. Geonor thermoelectric cooling control unit, model e-600
4. 2 Keithley digital multimeters, model 177
5. Keithley digital multimeter, model 191
6. Keithley digital multimeter, model 160
7. Hewlett Packard twin channel d.c. power supply, model 6205B
8. Rikadenki zero suppression voltage unit, model SV-D
9. Canlab twin channel strip-chart recorder, model 285
10. 4 Kulite pressure transducers, model VQS-250 (rated pressure 50 psi)
11. Canlab single channel strip-chart recorder, model 255
12. 1 Kulite pressure transducer, model XTM-1-190 (rated pressure 100 psi)
13. 7 YSI 3000 Ω precision thermistors, model 44030
14. Sola Basic (single phase, 60 Hz, 120 volt) voltage regulator, model 63-13-210
15. Minolta camera and multifunction back, model X-700 (film, panatomic-x ASA 32)
16. 2 Hammond 125 V power bars, cat. no 1584 H8A
17. 2 Boxer 115 V fans, model WS2107 FL-1002
18. 2 Triple-channel switching units
19. 1 Multi-channel switching unit
20. 10 Whitey stainless-steel ball valves, model 42S4
21. 4 Nupro brass v-stem valves, model 4-J